Doctoral Thesis

^{137}Cs Migration from Sloped Forest Catchment to Water Body and Its Contribution to Air Dose Rate

(傾斜森林集水域から水域への ^{137}Cs の移行とその空間線量率への寄与)

2020

Triyono Basuki
D174706

Department of Chemistry
Graduate School of Science
Hiroshima University

List of Publications

1. **Air dose rate to ^{137}Cs activity per unit area ratio for different land use 7 years after the nuclear accident -Case of the slope catchment, Ogi reservoir, Fukushima-**

   T. Basuki, W. C. Bekelesi, M. Tsujimoto, S. Nakashima

   Radiation Measurements (2020).
   https://doi.org/10.1016/j.radmeas.2020.106424.

2. **Examination of Cs tolerant bacteria interaction with Cs^{+} in aqueous solution and soil by using ^{137}Cs tracer**

   T. Basuki, K. Inada, S. Nakashima

   AIP-CP, accepted (2020).

3. **Investigation of radiocesium migration from land to waterbody using radiocesium distribution and soil to sediment ratio: A case of the steep slope catchment area of Ogi reservoir, Kawauchi Village, Fukushima**T. Basuki, W. C. Bekelesi, M. Tsujimoto, S. Nakashima

   Radiation Safety Management, **19**, (2020) 23-34. DOI 10.12950/rsm.190924

4. **Deposition Density of ^{134}Cs and ^{137}Cs and Particle Size Distribution of Soil and Sediment Profile in Hibara Lake Area, Fukushima: an Investigation of ^{134}Cs and ^{137}Cs Indirect Deposition into Lake from Surrounding Area**

   T. Basuki, S. Miyashita, M. Tsujimoto, and S. Nakashima

   Journal of Radioanalytical and Nuclear Chemistry, 316 (2018) pages1039–1046. DOI 10.1007/s10967-018-5809-1

Contents

Chapter VI Air dose rate to ^{137}Cs ratio for predicting future air dose rate derived from ^{137}Cs inventory …… 84

Chapter I

General Introduction

I-1. Background of study

The Fukushima Daiichi Nuclear Power Plant (FDNPP) accident that occurred on March 15, 2011, caused a substantial amount of radioactive materials released to the environment. Among the radioactive materials released to the environment, radiocesium (^{134}Cs and ^{137}Cs) having boiling point 670.8°C is the most major released radionuclide beside radioiodine (^{131}I), thus it has the most impact to land contamination.1) The longer ^{137}Cs half-life (30.2 years) in comparison to ^{134}Cs (2.06 years) and ^{131}I (8 days) has made the ^{137}Cs as the main radionuclide of interest to be studied.

Forest area covers more than 60% of the contaminated zone in Fukushima and it has higher radiocesium inventory in comparison to the other land use. 2,3) It has been known that forest retained the radioactive contamination strongly after the FDNPP accident, even in sloped area. Forest will be the area that has high contamination and high air dose rate for long time, that is a disadvantage, as forest is one of source of food. Furthermore, forest can be source of radioactive particulate contamination for lower areas like water body (river, lake, reservoir etc.) that can contaminate water resource. The soil-water body migration from forest catchment will be the main feature of radiocesium migration in Fukushima in the future.

The retention of radiocesium in soil has been investigated widely. It was due to strong adsorption of Cs by soil which was shown by its higher distribution coefficient value (Kd value) than some other elements.4) One of the reasons is relatively lower hydration enthalpy of Cs, in comparison with such as the other alkali elements. Fine particle of soil especially clay mineral also has been investigated to immobilize Cs, and trap Cs at its interlayer space.5)

Especially in the forest area, it has been shown that radiocesium was penetrated deeply in soil of forest than that of more open area, due to the role of litter layer and organic matter rich soil of forest area, even though the litter layer was also capable to retain the radiocesium.6) Radiocesium will be relatively strongly immobilized when it reaches the mineral soil layers of forest.3)

The understanding of radiocesium migration behavior is key to the assessment for the long-term radiation hazard risk and its countermeasures. However, there is still a question about why radiocesium is still strongly retained in forest area sometime after the accident, even in very steep sloped forest. The factors that influence the radiocesium migration from forest catchment to water body also still need to be investigated further. Furthermore, an easier method to investigate radiocesium migration from catchment to water body as well as an alternative method to estimate air dose rate derived from radiocesium in the future is very important to be developed. This method is important for evaluation of decontamination activity and for prediction of future air dose rate derived from ^{137}Cs inventory in the soil.

I-2. Research questions

I-2.1. How are the ^{137}Cs retention in sloped forest catchment and migration from sloped forest catchment to water body after 7 years?

I-2.2. How to analyze ^{137}Cs migration to water body?

I-2.3. How ^{137}Cs contributes to air dose rate in the future?

I-3. Hypotheses

I-3.1. ^{137}Cs retention in sloped forest catchment and migration from sloped forest catchment to waterbody are influenced by a mixture of physical, chemical and biological factors.

I-3.2. Ratio of ^{137}Cs in soil of catchment to ^{137}Cs in sediment is related to the time after FDNPP accident so that it is time dependent, it can be used to investigate the ^{137}Cs migration in future.

I-3.3. Ratio of Air dose rate to ^{137}Cs in soil of catchment can be used to estimate the future dose rate.

I-4. Research objectives

I-4.1. Investigate the influence of slope, type of area (forest type, non-forest), soil physicochemical property and soil microorganism in ^{137}Cs migration.

I-4.2. Calculation of ^{137}Cs in soil to sediment ratio and compare it with some previous researches for investigation of ^{137}Cs migration.

I-4.3. Calculation of Air dose rate to ^{137}Cs in soil ratio for estimating the future air dose rate.

I-5. References

1) IAEA (2015) The Fukushima Daiichi Accident. FUKUSHIMA DAIICHI Accid. Tech. Vol. 1
2) Laceby, J. P., Huon, S., Onda, Y., Vaury, V., Evrard, O., Journal of Environmental Management, 2016, 183, Part 3, P 742-753. https://doi.org/10.1016/j.jenvman.2016.09.020.
3) Kurihara, M., Onda, Y., Kato, H., Loffredo, N.,Yasutaka, T., Coppin, F., Journal of Environmental Radioactivity, 2018, 187, 81-89. https://doi.org/10.1016/j.jenvrad.2018.01.027.
4) Markert B., and Friese K., Trace element, their distribution and effects in the environment, Elsevier, 2000.
5) Bostick B. C., Vairavamurthy M. A., Karthikeyan K. G., Chorover, Journal of Environmental Science and Technology, 2002, 36:2670–2676. doi: 10.1021/es0156892.
6) Koarashi, J., Andoh, M. A., Matsunaga, T., Sato, T., Nagao, S., Nagai, H., The Science of Total Environment, 2012, 431, 392–401. https://doi:10.1016/j.scitotenv.2012.05.041.

Chapter II

Air dose rate measurement, soil and sediment sampling and Measurement[1,2]

---

[1] Investigation of radiocesium migration from land to waterbody using radiocesium distribution and soil to sediment ratio: A case of the steep sloped catchment area of Ogi reservoir, Kawauchi Village, Fukushima

T. Basuki, W. C. Bekelesi, M. Tsujimoto, S. Nakashima, *Radiation Safety Management*, 19, (2020) 23-34. DOI 10.12950/rsm.190924

[2] Air dose rate to ^{137}Cs activity per unit area ratio for different land use 7 years after the nuclear accident -Case of the sloped catchment, Ogi reservoir, Fukushima-

T. Basuki, W. C. Bekelesi, M. Tsujimoto, S. Nakashima, *Radiation Measurements* (2020). https://doi.org/10.1016/j.radmeas.2020.106424.

II-1. Study area and period

The study area is in Ogi reservoir catchment area, Kawauchi village, Fukushima, that is located about 18 km southwest from FDNPP. It is one of the areas that were passed by the radioactive plum following the FDNPP accident, thus the area received a significant amount of radioactive material. There have been various researches about radioactive contamination and its consequences in this area.[1,2] Air dose rate measurement sites were selected purposively that consist of forest area, transition zone (no vegetation) and farmland of the catchment area. The soil sampling sites were selected purposively within each air dose rate measurement area as an imaginary transect 2 x 2 m^2. Sediment core samples were collected from the deeper part and most ^{137}Cs contaminated area of the reservoir based on the previous study.[3] The study area is shown in Figure II-1.1 and details of air dose measurement and sampling area are shown in Table II-1.1 and II-1.2. Air dose measurement and soil and sediment core sampling were conducted during March 15~16, 2018.

II-2. Air dose rate measurement

The ambient equivalent dose rate in air (air dose rate) was measured by survey meter with NaI detector (ALOKA MYRATE PDR-111) 1 m above the ground. The survey meter has been periodically calibrated using standard source and standard survey meter. Geographic position and elevation of the sites were recorded using GPS locator (Garmin, Oregon 650TCJ).

II-3. Soil and sediment sampling and sample treatment

The soil sample was collected by hand core sampler (25 cm long tube, 19.6 cm^2 area) and the sediment sample was collected by gravity core sampler (6.5 cm diameter and 60 cm long tube). Geographic position and elevation of the sites were recorded using GPS locator (Garmin, Oregon 650TCJ). Soil and sediment samples were sent to laboratory by maintaining the vertical profile. The soil sample and sediment sample were cut 2 cm each and 1 cm each, respectively, dried at room temperature for 1 day and further oven dried at 105°C for about 1 day. The soil was sieved by horizontal rotating sieve (SKH-01, AS ONE) with 2 mm sieve at about 100 rpm to separate stone and gravel from the sample. The soil sample with size < 2 mm was packed into so called U8 vessel (100 ml, 5 cm height, 5 cm diameter).[4] For terrestrial natural gamma emitter radionuclides (TNRs) measurement, the soil sample was sealed and kept for about 3~4 weeks prior to the measurement.

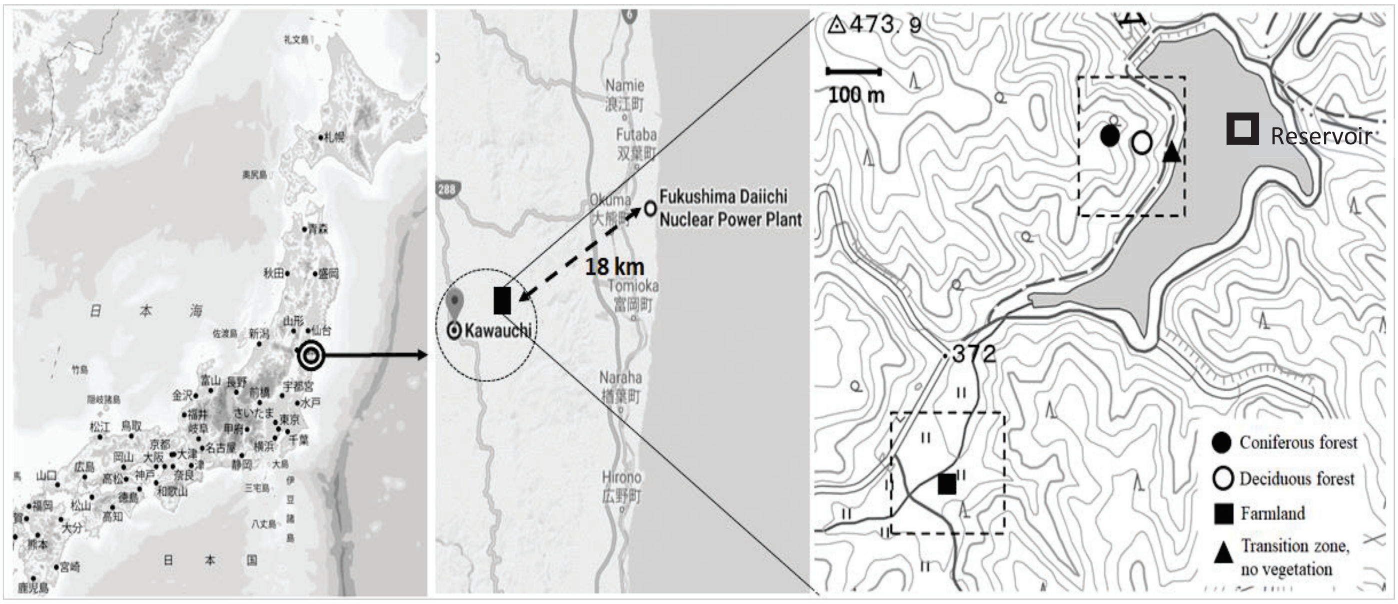

Figure II-1.1. Location of air dose rate measurement and soil and sediment sampling, Kawauchi Village, Fukushima.

Table II-1.1. Details information of the sampling site in Ogi reservoir area, Kawauchi Village, Fukushima

Area	Samples	Location		Elevation (m)	Core sample depth (cm)	Site details
		Latitude (N)	Longitude (E)			
Area 1	1	37.34363	140.90566	378	0~18	The sampling area is in the middle to the top of the ridge, consisted of mixed forest between coniferous and deciduous forest type.
	2	37.34359	140.90571	376	0~18	
	3	37.34372	140.90567	379	0~16	
	4	37.34365	140.90559	382	0~18	
Area 2	1	37.34364	140.90589	369	0~20	The sampling area is in the middle of the ridge, consisted of mixed forest between coniferous and deciduous forest type.
	2	37.34363	140.90589	369	0~20	
	3	37.34368	140.90589	368	0~21	
Area 3	1	37.34362	140.90615	365	0~20	The sampling area is in between the catchment and reservoir or transition zone, there is no vegetation.
	2	37.34361	140.90613	365	0~20	
	3	37.34357	140.90623	365	0~7	
Area 4	1	37.33924	140.90168	372	0~20	Farmland located in the upper area of catchment, close to river
	2	37.33924	140.90169	372	0~20	
	3	37.33924	140.90170	372	0~20	
Reservoir	1	37.34426	140.90716	362	0~35	The sampling area is in the deep area of the reservoir
	2	37.34426	140.90716	362	0~35	

Table II-1.2. Location of air dose measurement site

Area	Measurement	Location		Elevation (m.a.s.l)
		Latitude (N)	Longitude (E)	
Area 1, forest	1	37.34359	140.90571	376
	2	37.34363	140.90566	378
	3	37.34363	140.90565	378
	4	37.34372	140.90567	379
	5	37.34364	140.90542	389
	6	37.34358	140.90554	383
	7	37.34365	140.90559	382
	8	37.34369	140.90559	382
	9	37.34376	140.90550	389
	10	37.34380	140.90549	391
	11	37.34388	140.90543	394
Area 2, forest	1	37.34368	140.90589	368
	2	37.34356	140.90592	368
	3	37.34367	140.90588	369
	4	37.34364	140.90589	369
	5	37.34363	140.90589	369
Area 3, no vegetation	1	37.34354	140.90634	365
	2	37.34370	140.90617	365
	3	37.34356	140.90628	365
	4	37.34357	140.90623	365
	5	37.34358	140.90620	365
	6	37.34362	140.90615	365
	7	37.34361	140.90613	365
Area 4, Farmland	1	37.33924	140.90168	372

m.a.s.l shows meter above sea level.

II-4. ^{134}Cs, ^{137}Cs and terrestrial natural gamma emitter radionuclides (TNRs) measurement

The radioactivity of radionuclide from fallout (^{134}Cs, ^{137}Cs) and TNRs, which are ^{238}U decay series, ^{232}Th decay series and ^{40}K, were measured by gamma spectrometer with low background HP Ge detector (GEM 30-70, ORTEC), see Figure II-3.1. The gamma energy 604 keV, 662 keV and 1460 keV were used for determining the concentration of ^{134}Cs, ^{137}Cs and ^{40}K, respectively. For the ^{238}U decay series, ^{214}Pb (295, 351 keV) and ^{214}Bi (609, 1120 keV) were measured. For ^{232}Th decay series, ^{228}Ac (338, 911 keV), ^{208}Tl (583, 860 keV), ^{212}Pb (238.6 keV) and ^{212}Bi (727,3 keV) were measured. The measurement especially for U-238 and Th-232 decay series was conducted about 48 hours for each sample. The measurement is judged to be sufficient when the measurement error value reached less than 10%.

Counting efficiency was calibrated using a set of standard sources (MX033U8PP) manufactured by Japan Radioisotope Association, see Figure II-3.2, II-3.3 and II-3.4. The activity concentration and inventory of radionuclides (activity per unit area) were calculated using equation (1) and (2), respectively. The calculated activity concentration and inventory were decay corrected to the sampling day.

$$A = N/(\varepsilon \bullet I\gamma \bullet m) \qquad (1)$$

where A activity concentration (Bq/kg), N net counts per second (CPS) = $\mathrm{CPS_{sample}}$ – $\mathrm{CPS_{background}}$, ε gamma spectrometer counting efficiency resulted from the calibration, $I\gamma$ emission rate of selected gamma ray, m mass of the soil sample (kg).

$$I = A \bullet M \qquad (2)$$

where I radionuclide inventory (Bq/m^2), A activity concentration (Bq/kg) and M cumulative mass of soil sample (kg/m^2).

The detection limit of gamma ray spectrometer was calculated by considering the background measurement and measurement time by following previous research.[5]

The contribution of terrestrial natural gamma ray emitter radionuclides (TNRs) to the air dose rate was evaluated. The activity concentration (Bq/kg) of natural radionuclides was converted to air kerma rate (nGy/h) by using dose coefficient 0.623 (nGy/h)/(Bq/kg) for ^{232}Th series, 0.461 (nGy/h)/(Bq/kg) for ^{238}U series and 0.0414 (nGy/h)/(Bq/kg) for ^{40}K.[6] Ambient dose equivalent rate was calculated by considering ambient dose equivalent dose rate to air kerma rate ratio was 1.2 for natural gamma rays.[7]

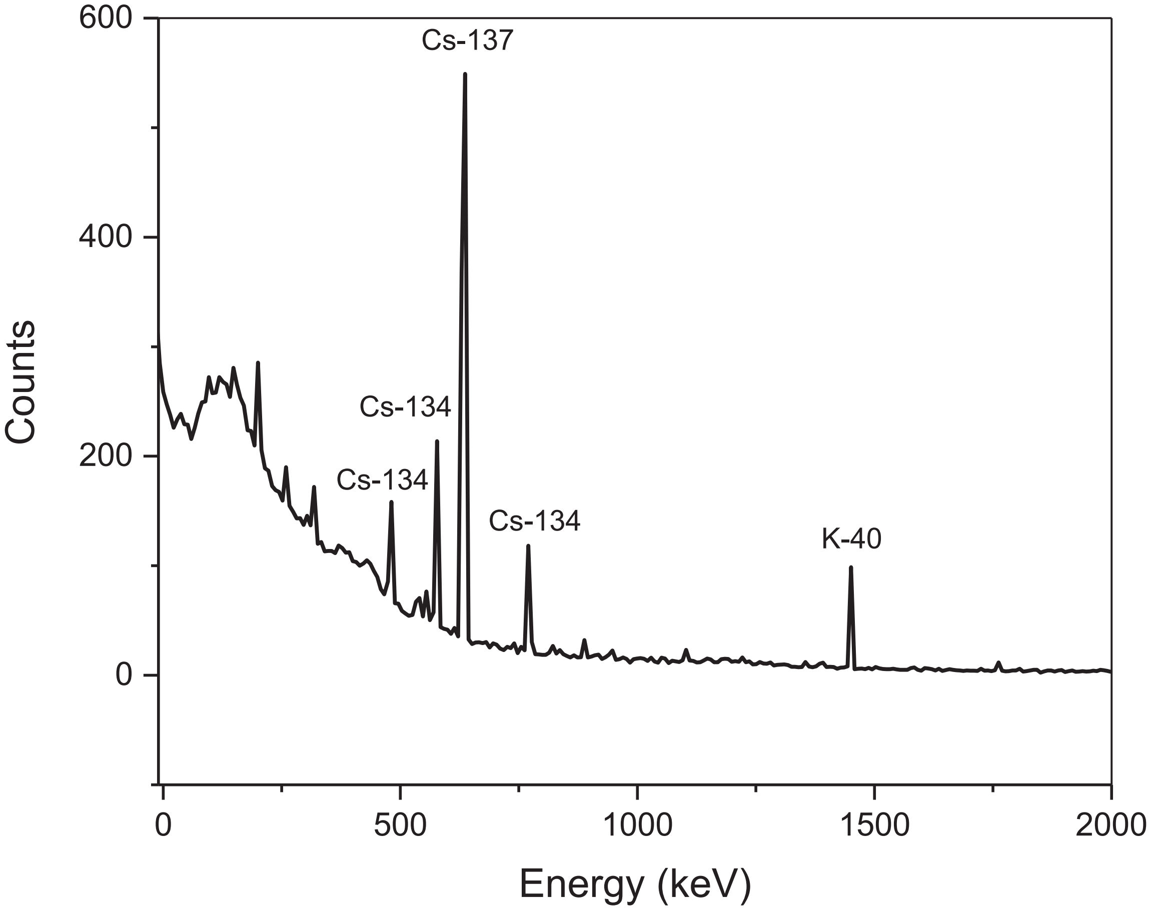

Figure II-3.1. Typical gamma energy spectrum of some radionuclides in the sample.

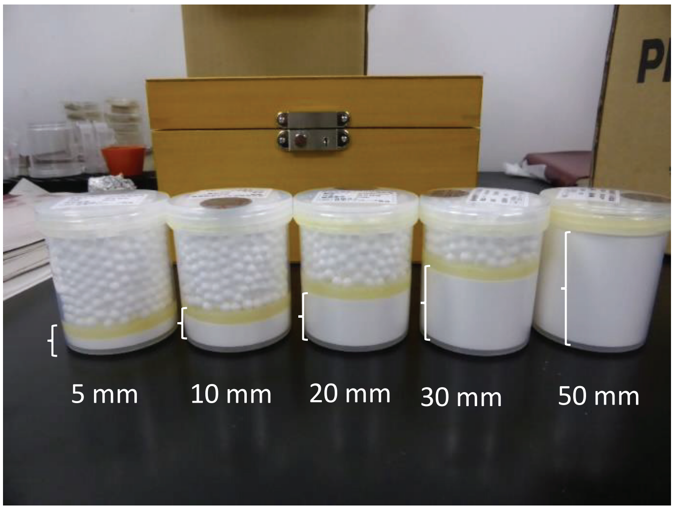

Content of sample	
Radioisotopes	Eɣ (keV)
Cd-109	88.03
Co-57	122.06
	136.47
Ce-139	165.85
Cr-51	320.08
Sr-85	513.99
Cs-137	661.65
Mn-54	834.83
Y-88	898.02
Co-60	1173.24
	1332.5
Y-88	1836.01

Figure II-3.2. Standard source with different sample thickness for calibration of gamma spectrometer.

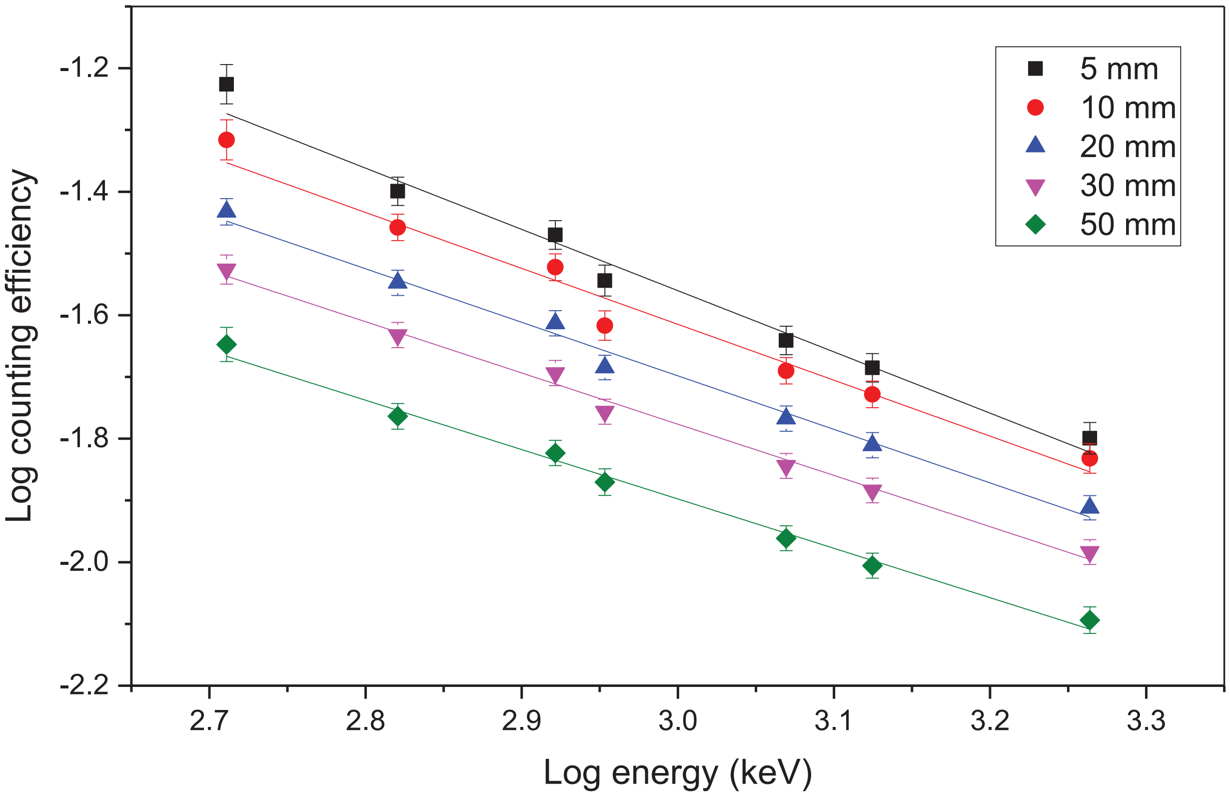

Figure II-3.3. Counting efficiency of gamma spectrometer resulted from standard source measurement for medium to high energy region of gamma ray.

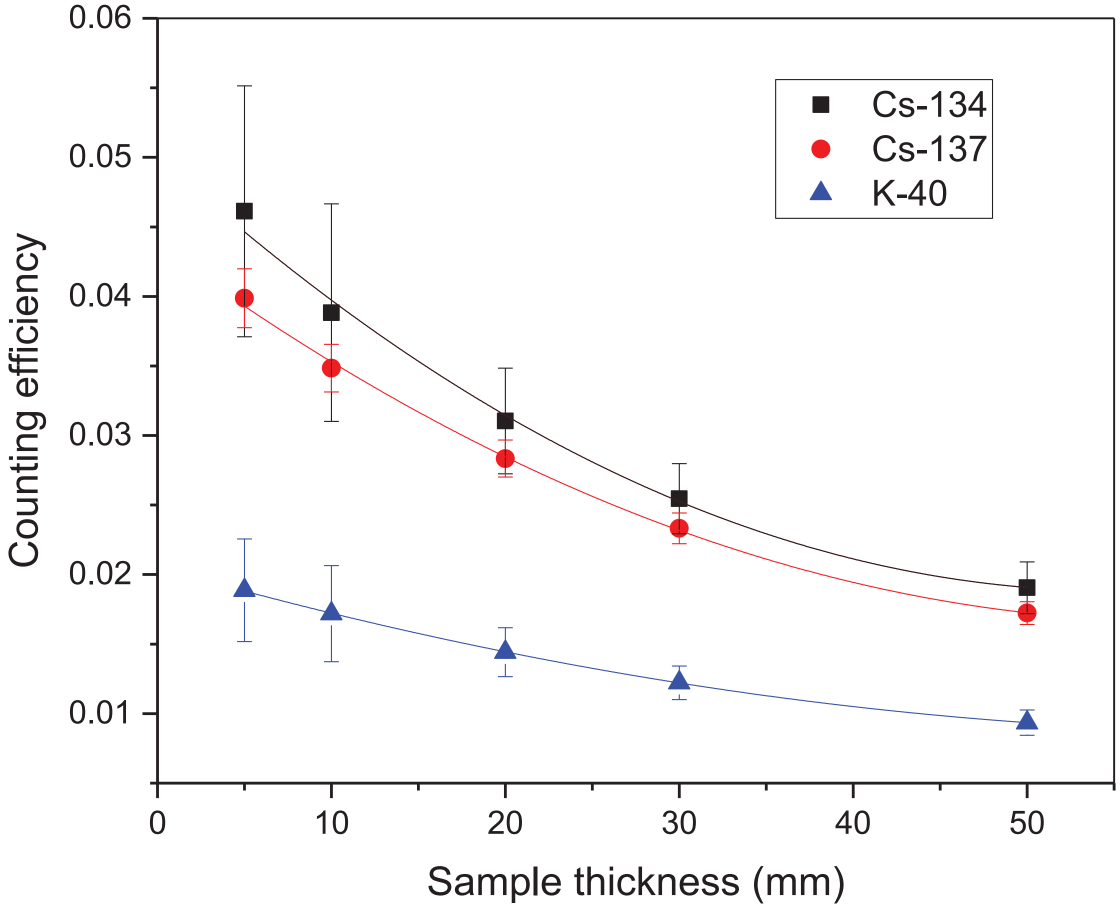

Figure II-3.4. Counting efficiency of gamma spectrometer for some radionuclides in the samples having different thickness.

II-5. Soil physicochemical property analysis

II-5.1. Particle size characterization

The samples were dried at room temperature for 24 hours and further dried by oven at 105 ºC for 24 hours to remove water content thoroughly. The dried core samples were sieved by electric horizontally rotating sieve, SKH-01, AS ONE, with mesh size 2 mm at about 280 rpm for 1 hour to separate stone and coarse particle from finer particle. It was further sieved by using sieve with mesh size 75 μm at about 280 rpm for 3 hours to separate sand from silt and clay particle. The particle size characterization of samples in more detail followed previous work.[4]

II-5.2. Soil pH

Soil pH was measured by measuring the pH of soil sample-distilled water mixture (1/5 of w/v ratio), as previous work.[8] The soil sample and distilled water were mixed by vortex for about 2 minutes and soil slurry was measured using pH meter.

II-5.3. Organic matter (OM) content

Organic matter (OM) content fraction was determined by weight loss on ignition method according to the previous work.[9] The samples were placed in funnel furnace (FO300, Yamato scientific) at 500°C for 12 hours after conducting the soil pre-treatment.

II-5.4. Cation exchange capacity (CEC)

The major exchangeable cations and cation exchange capacity (CEC) of surface soil sample were determined by NH_4^+ exchange (1 M Ammonium acetate, pH 7, 1/5 of w/v ratio), as previous research. [8, 10] The concentration of extracted cations was measured by ICP AES spectrometry (SPS3500, Hitachi). The precipitate of exchangeable cation measurement was used to determine the CEC, by extracting the NH_4^+ ion on soil matrix by using 1 M KCl. The CEC of the soil was determined as the concentration of ammonium ion released into the supernatant. The extracted NH_4^+ concentration was measured by colorimetry (Methyl red, Thymol blue and titration of 0.01 M NaOH).

II-5.5. Base saturation

The base saturation was calculated based on the ratio of total exchangeable cation to CEC.

II-6. References

1 Taira, Y. et al., PLoS ONE, 2012, 7(9): e45816.

2 Tsuchiya, R. et. al, PLoS ONE, 2017, 12(12):e0189398.

3 Funaki, H. et al., Material Research Society Symposium Proceeding. Vol. 1665 (2014).

4 Tsujimoto M., Miyashita S., Nguyen H.T., Nakashima S., Radiation safety management, 2016, 15:1–4. doi: 10.12950/rsm.160107

5 Cooper, J. A., Nuclear Instrument and Method, 1970, 82, 273-277.

6 UNSCEAR, 1993, New York, USA.

7 Mikami, S. et al., 2019, Journal of Environmental Radioactivity, 210, 105941. https://doi.org/10.1016/j.jenvrad.2019.03.017.

8 Fujii, K. et. al, Soil science and plant nutrition, 60, 751-764 (2014).

9 Kettler, T. A. and Doran J. W., Soil science Society of America Journal, 65:849-852 (2001).

10 Koarashi, J. et. al, The science of total environment 43:392-401 (2012).

Chapter III

Initial study of ^{137}Cs migration in Hibara Lake[1]

[1] Deposition Density of ^{134}Cs and ^{137}Cs and Particle Size Distribution of Soil and Sediment Profile in Hibara Lake Area, Fukushima: an Investigation of ^{134}Cs and ^{137}Cs Indirect Deposition into Lake from Surrounding Area

T. Basuki, S. Miyashita, M. Tsujimoto, and S. Nakashima, *Journal of Radioanalytical and Nuclear Chemistry,* 316 (2018) pp 1039–1046. DOI 10.1007/s10967-018-5809-1

III-1. Introduction

^{134}Cs and ^{137}Cs contaminant in environment has been a high concern after the Fukushima Daiichi Nuclear Power Plant (FDNPP) accident which occurred on March 15, 2011 in Fukushima, Japan. It is due to relatively long half-life of ^{134}Cs and ^{137}Cs which is 2.06 years and 30.17 years, respectively, and ^{134}Cs and ^{137}Cs are the most major released radionuclide during the accident in addition to the radioactive iodine (I-131).[1]

Deposition process of released ^{134}Cs and ^{137}Cs into water body (direct deposition from atmosphere and indirect or secondary deposition from catchment area) has been widely investigated.[2,3] The indirect deposition of ^{134}Cs and ^{137}Cs into water body from catchment after the nuclear accident is a long-term process. In the beginning, the main fraction of ^{134}Cs and ^{137}Cs that migrated to lake from catchment was a dissolved form which occurred in short period of time after FDNPP accident. In longer period, the ^{134}Cs and ^{137}Cs that migrated to lake were mostly incorporated with soil particle especially fine particle such as clay minerals.[4-6]

Depth profile of ^{134}Cs and ^{137}Cs in lake sediment has been well considered as information for determination of age of sediment as well as to understand the sedimentation process.[7,8] By assuming that the ^{134}Cs and ^{137}Cs peak at certain layer of sediment was temporally dependent, the depth profile corresponds to certain event such as global fall out from atomic bomb test and FDNPP accident.

The study aimed to investigate the indirect deposition of ^{134}Cs and ^{137}Cs from catchment into lake. The idea is that the difference in depth dependence and location dependence tells indirect deposition. The sediment of shallow area of lake was used in this research instead of deep area of lake. Deposition density of ^{134}Cs and ^{137}Cs in each sediment layers was measured. Particle size distribution was measured by sieving and ^{134}Cs and

^{137}Cs activity concentration in each size fraction was also measured. The depth profile of ^{134}Cs and ^{137}Cs in flat and sloped area was compared to analyze the indirect deposition process of ^{134}Cs and ^{137}Cs from specific area of lake catchment.

III-2. Study area, Soil and sediment sampling and experimental method

III-2.1. Study area and period

Core samples were taken from the Hibara Lake that is located in Yama gun, Fukushima prefecture about 100 km away from FDNPP. The Hibara Lake is part of Bandai-Asahi National park at 819 m altitude. It has 10.8 km^2 surface area, 12 m averaged depth and 0.83 year retention time.[9] Three areas were selected purposively which represent relatively flat area (area 1), sloped area (area 2) and high sloped area (area 3) of lake. In area 1, sampling points in shallow area of lake (L1-1, L1-2 and L1-3), river (R1-1, R1-2) and surrounding area (S1-1, S1-2) were chosen in order to investigate complex process of indirect deposition that may occur due to the influence of river. Sampling points in Area 2 (L2-1, L2-2) and Area 3 (L3-1, L3-2) are only in shallow area of lake without river influence. Sampling sites are shown in detail in Figure III-2.1 and Table III-2.1. Soil and sediment samples were collected on August 8 to 9, 2016, by employing hand core sampler.

III-2.2. Soil and sediment sample treatment and ^{134}Cs and ^{137}Cs measurement

The core samples were sliced by each 5 cm, the weight was measured, and it was packed in plastic vessel, called U-8 vessel. Activities of ^{134}Cs and ^{137}Cs of bulk samples were measured by using gamma spectrometer with high purity Ge semiconductor detector, GEM 30-70, ORTEC. The energy peak of 605 KeV and 662 KeV were used for detection of ^{134}Cs and ^{137}Cs, respectively.

Furthermore, the bulk samples were dried at room temperature for 24 hours and further dried by oven at 105 ºC for 24 hours to remove water content thoroughly. The dried core samples were sieved by electric horizontally rotating sieve, SKH-01, AS ONE, with mesh size 2 mm at about 280 rpm for 1 hour to separate stone and coarse particle from finer particle. It was further sieved by using sieve with mesh size 75 µm at about 280 rpm for 3 hours to separate sand from silt and clay particle. Sand particle and silt and clay particle of sample were packed in U8 vessel separately. The activity concentrations of ^{134}Cs and ^{137}Cs in sand and silt and clay component of soil and lake sediment were measured in the same way with bulk sample and compared.

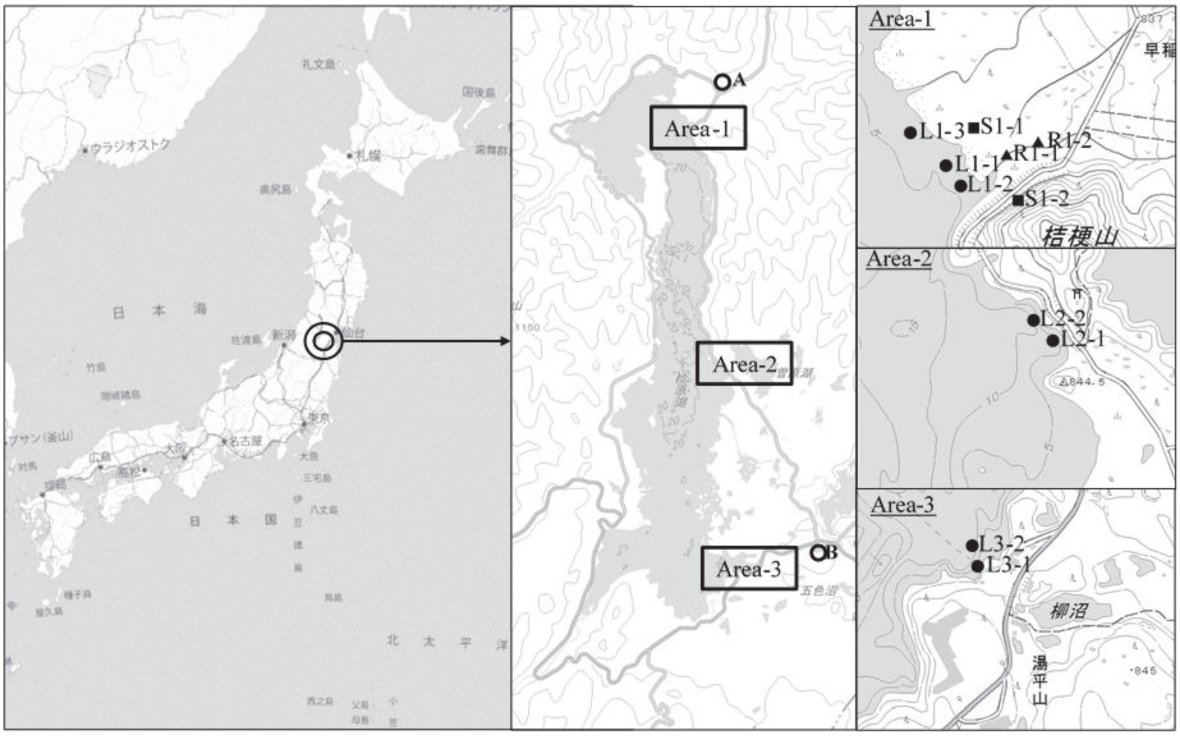

Figure III-2.1. Research area and sampling points. L: Lake Sediment, S: Soil, R: River sediment, A and B are the area where Japanese Government measured radioactivity on March, 2012. Cs-134 and Cs-137 at point A are 15,000 Bq/m^2 and 20,000 Bq/m^2, respectively, at point B are 66,000 Bq/m^2 and 86,000 Bq/m^2, respectively.

Table III-2.1. Details information of sampling site

	Area	Samples	Location		Altitude (m a.s.l)	Site Description
			Latitude (N)	Longitude (E)		
Area 1	Shallow area of lake close to the edge, relatively flat area	L1-1	37.722032	140.057528	821	close to river mouth, 20 cm water depth
		L1-2	37.72168	140.057817	821	close to river mouth, 30 cm water depth
		L1-3	37.722964	140.056293	821	relatively far from river mouth, 30 cm water depth
	River	R1-1	37.722209	140.058901	830	30 cm water depth
		R1-2	37.722273	140.05907	832	30 cm water depth
	Surrounding Area	S1-1	37.722704	140.057681	825	flat surrounding area
		S1-2	37.721813	140.05894	832	sloped surrounding area
Area 2	Shallow area of lake close to the edge, relatively high sloped area	L2-1	37.684398	140.065247	821	no river, 50 cm water depth
		L2-2	37.68451	140.065211	821	no river, 60 cm water depth
Area 3		L3-1	37.653633	140.064382	822	no river, 50 cm water depth
		L3-2	37.65367	140.064375	821	no river, 100 cm water depth

m a.s.l. shows meter, above sea level.

III-3. Results and discussion

Radioactivity concentrations of ^{134}Cs and ^{137}Cs which were corrected at released day, March 15, 2011 were summarized in Table III-3.1. The ^{134}Cs and ^{137}Cs were detected in all sampling points. Ratio between the concentrations of ^{134}Cs and ^{137}Cs was about 1. This ratio value was in good agreement with reported value of radionuclide inventory of FDNPP at the time of accident. This result means that the ^{134}Cs and ^{137}Cs in sediment profile was derived from Fukushima accident.[1)]

Results of sieving are presented in Table III-3.1. In general, the main fraction of all samples was sand which was about 40 ~ 82%, except for sample L3-2 where gravel was the most dominant fraction. Difference among samples was in gravel and silt and clay fraction content. In lake sediment samples, there was a variation of gravel and silt and clay fraction proportion. Whereas in river sediments, there was always higher proportion of gravel (23% ~ 55 %) and smaller proportion of silt and clay fraction (< 4%). To the contrary, the soil samples have lesser gravel (< 9%) and have higher proportion of silt and clay fraction (11% ~ 37%) than river and lake sediment samples.

Comparison of particle size distribution data between sediment and soil might explains the particle transport from catchment to lake. Sediment of river showed very poor fine particle content. It was washed away by current to the river mouth and lake. In the case of lake sediment area 1, sediment located closer to river mouth (L1-1 and L1-2) has poorer silt and clay content. While, in general the silt and clay content of lake sediment was larger than river sediment but lesser than soil, except L1-1 and L3-2. It probably showed that silt and clay that migrated from catchment were slightly accumulated in shallow area sediment. The variation of silt and clay content of lake sediment probably showed the occurrence of horizontal redistribution.

Figure III-3.1. shows depth profile data of ^{134}Cs and ^{137}Cs deposition density in shallow area of lake sediment samples. The data are decay corrected at sampling day, August 8, 2016. ^{134}Cs and ^{137}Cs in general were mainly deposited on the surface (0-10 cm) of lake sediment in all sediment samples. This tendency is in line with previous researches result on vertical profile of ^{134}Cs and ^{137}Cs in Fukushima Lake and reservoir.[6, 10-11] Such tendency has been investigated widely that was due to strong adsorption of ^{134}Cs and ^{137}Cs that deposited in lake, either atmospheric-derived or catchment-derived ^{134}Cs and ^{137}Cs, by solid particle of sediment. While the tail under the peak layer probably showed small fraction of downward post depositional redistribution due to diffusion and mixing by biological process.

Figure III-3.1 furthermore showed that there was a slightly different vertical depth profile between samples collected from flat and sloped areas. ^{134}Cs and ^{137}Cs on sediment samples of flat area (area 1) were always deposited mainly at 0-5 cm depth. Whereas, the peak of ^{134}Cs and ^{137}Cs on sediment samples of sloped area (area 2 and 3) was at 5-10 cm depth, except for sample L3-2. The difference in depth profiles of ^{134}Cs and ^{137}Cs probably showed that the sedimentation rate or indirect deposition rate in lake was faster in the area near steep-sloped catchment. It was also indicated that steep sloped area contributed to larger influx of sediment and ^{134}Cs and ^{137}Cs than in flat area. It is supported by previous research which shows slower indirect deposition or secondary deposition in flat area.[6] However, the accumulation of ^{134}Cs and ^{137}Cs at deeper layer of sediment in sloped area was also possible as a result of mudslide due to steep slope.

Moreover, the deposition densities of ^{134}Cs and ^{137}Cs on lake sediment samples in area 1 decay corrected at sampling day August 8, 2016 are lower than the deposition density of soil in surrounding area sampling point A that was measured by Japanese government on March, 2012. On the other hand, the deposition density of lake sediment in Area 3 sample L3-1 is higher than the deposition densities of soil in surrounding area sampling point B. It can be said that accumulation of catchment-derived Cs-134 and Cs-137 beyond river system occurred in near steep sloped area.

Different pattern of deposition density was found in area 3 compared to area 2, although both are categorized as steep sloped area (see Figure III-3.1.). In area 3, peak layer of L3-2 sample was at 0-5 cm depth, which is similar with that in flat area. In addition, the deposition density of ^{134}Cs and ^{137}Cs in L3-2 was much order smaller than in L3-1. These are probably due to the fact that L3-2 sample was taken from area that was slightly deeper area and has more distance to edge of the lake than L3-1. This might suggest that the ^{134}Cs and ^{137}Cs which migrated from surrounding area to the lake were easily trapped near edge of the lake (L3-1), therefore the ^{134}Cs and ^{137}Cs could not easily reach L3-2. This also showed a large spatial variation of ^{134}Cs and ^{137}Cs deposition density among sampling points, which was probably affected by horizontal redistribution.

Figure III-3.2. shows comparison of ^{137}Cs deposition densities on peak layer of soil in surrounding area, sediment of river and lake sediment in area 1, flat area. The deposition densities of lake sediment samples L1-1 and L1-2 that are closer to river mouth show a close value to deposition densities of river sediment samples and 2 folds magnitude lower than deposition densities of soil samples. To the contrary, the deposition density in lake sediment L1-3 that is relatively far from river mouth is about five folds magnitude less than deposition densities of river sediment and extremely lower than deposition densities of soil samples. This finding probably revealed that the catchment-derived ^{134}Cs and ^{137}Cs in lake near flat area were mainly from river system which differs from lake sediment near steep sloped area.

Activity concentration of ^{134}Cs and ^{1377}Cs on sand fraction and silt and clay fraction of lake sediment and soil are summarized in Table III-3.2. The activity concentration of ^{134}Cs and ^{137}Cs was always higher on silt and clay fraction than on sand fraction.

Moreover, peak layer of soil and sediment samples were found always to have the highest activity concentration of ^{134}Cs and ^{137}Cs on silt and clay fraction. On the other hand, the silt and clay fraction that was obtained from sediment at upper or below the peak layer contained relatively less ^{134}Cs and ^{137}Cs.

The result has a good agreement with previous research that shows higher ^{134}Cs and ^{137}Cs adsorption capacity of fine particle particularly clay minerals.[10,11] It has been known well that in addition to the reason of wider surface area of finer particle to adsorb ^{134}Cs and ^{137}Cs ion either physically or chemically, clay mineral has specific adsorption site for ^{134}Cs and ^{137}Cs so call frayed edge site that can make ionic bonding with ^{134}Cs and ^{137}Cs cation.[12,13]

It also probably suggests that during indirect deposition process of ^{134}Cs and ^{137}Cs, silt and clay fraction was a medium of transportation through erosion process in surrounding area during rain fall. This finding is in line with previous researches that showed a dominant role of ^{134}Cs and ^{137}Cs incorporated with soil particle in ^{134}Cs and ^{137}Cs indirect deposition that depends on precipitation and geomorphological aspect of lake area. This finding also brings to information that probably the silt and clay at peak layer was from surface soil of surrounding area at the time of accident.

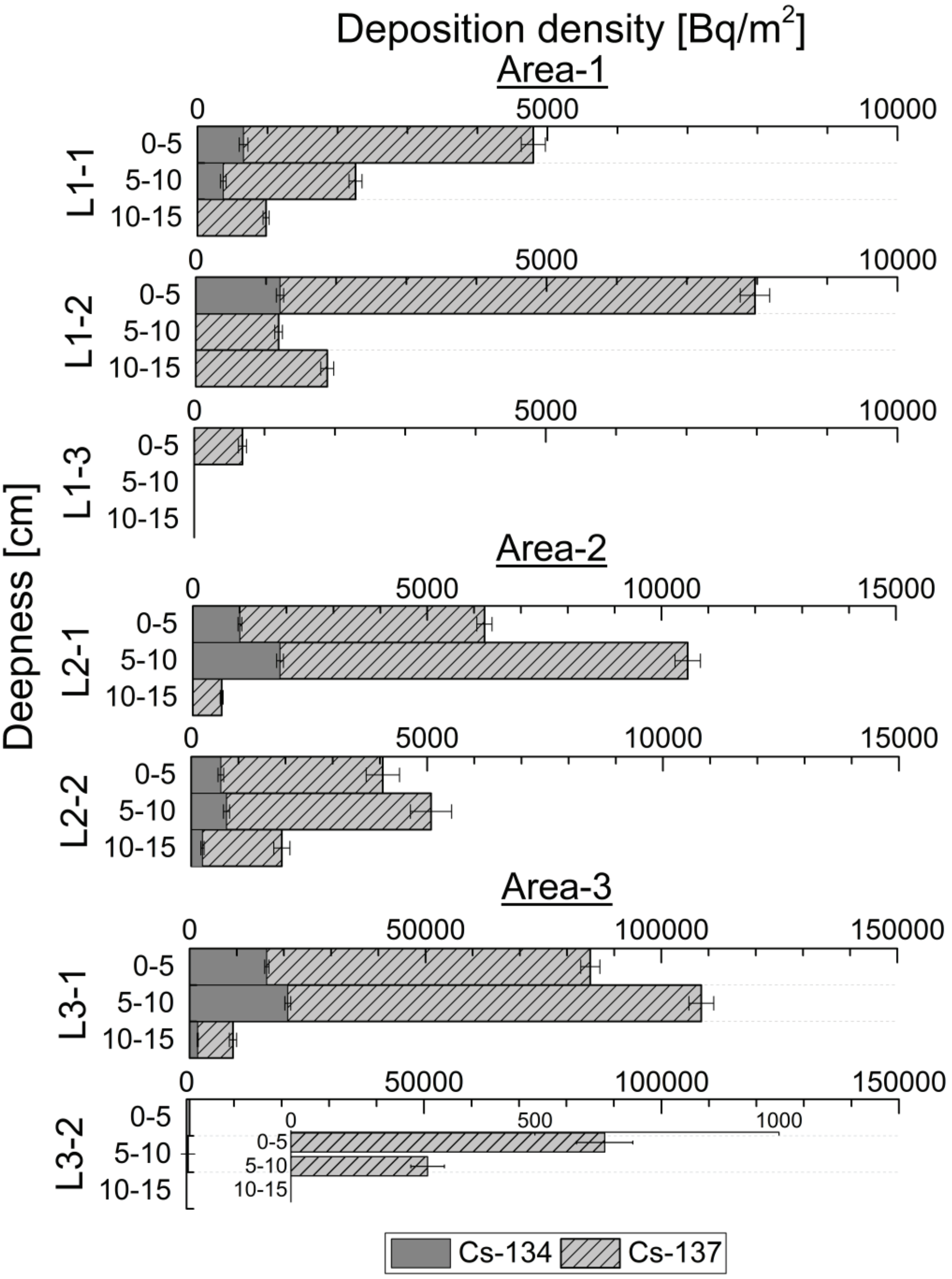

Figure III-3.1. Depth profile of deposition densities (Bq/m^2) of ^{134}Cs and ^{137}Cs in sediment, which are decay corrected at sampling day, August 8, 2016.

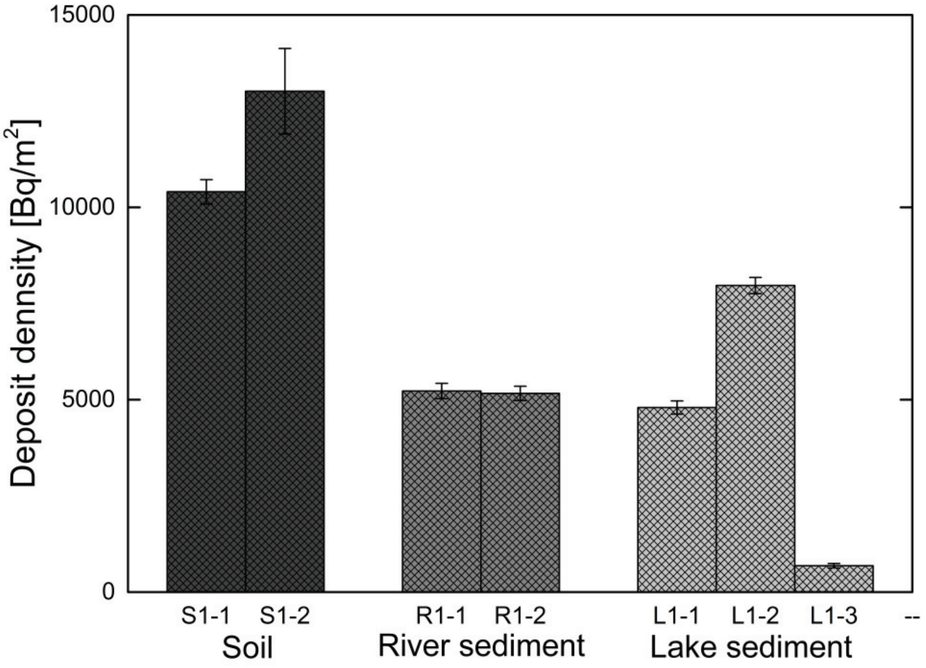

Fig III-3.2. Deposition densities (Bq/m^2) of ^{137}Cs in surface (0-5 cm) of soil in surrounding area, river sediment and lake sediment in Area 1 (flat area), which are decay corrected at sampling day, August 8, 2016.

Table III-3.1. Activity concentration of ^{134}Cs and ^{137}Cs (Bq/kg) and particle size distribution of sediment and soil samples

Samples		Deepness(cm)	^{134}Cs		^{137}Cs		Ratio ^{134}Cs/^{137}Cs	Particle Size Distribution		
								Gravel	Sand	Silt and Clay
			Bq/kg	error	Bq/kg	error		> 2mm	2 mm - 70 μm	< 70 μm
Lake Sediment	L1-1	0-5	59	2	78	3	0.76	0.47	0.49	0.04
		5-10	32	1	35	2	0.91	0.57	0.40	0.03
		10-15	<N.D.>		14	1	<N.A.>	0.31	0.64	0.05
	L1-2	0-5	104	3	126	3	0.83	0.18	0.66	0.16
		5-10	<N.D.>		18	1	<N.A.>	0.15	0.69	0.16
		10-15	<N.D.>		30	2	<N.A.>	0.04	0.72	0.24
	L1-3	0-5	<N.D.>		10	1	<N.A.>	0.02	0.63	0.35
		5-10	<N.D.>		<N.D.>		<N.A.>	0.03	0.52	0.45
		10-15	<N.D.>		<N.D.>		<N.A.>	0.01	0.51	0.48
	L2-1	0-5	86	2	96	3	0.90	0.22	0.60	0.18
		5-10	160	4	165	4	0.97	0.13	0.67	0.20
		10-15	<N.D.>		9.6	0.4	<N.A.>	0.32	0.55	0.13
	L2-2	0-5	93	8	110	10	0.85	0.42	0.54	0.04
		5-10	120	10	150	10	0.80	0.43	0.52	0.05
		10-15	31	3	45	4	0.69	0.43	0.43	0.14
	L3-1	0-5	1010	20	1150	30	0.88	0.34	0.61	0.05
		5-10	1380	30	1580	40	0.87	0.47	0.46	0.07
		10-15	410	30	480	40	0.85	0.31	0.56	0.13
	L3-2	0-5	<N.D.>		17	2	<N.A.>	0.74	0.25	0.01
		5-10	<N.D.>		7.2	0.9	<N.A.>	0.55	0.43	0.02
		10-15	<N.D.>		<N.D.>		<N.A.>	0.41	0.56	0.03
River Sediment	R1-1	0-5	65	3	75	3	0.87	0.32	0.64	0.04
		5-10	38	4	34	3	1.12	0.55	0.43	0.02
		10-15	<N.A.>		<N.A.>		<N.A.>			
	R1-2	0-5	66	2	78	3	0.85	0.23	0.75	0.02
		5-10	41	2	44	2	0.93	0.55	0.43	0.02
		10-15	82	7	82	7	1.00	0.26	0.70	0.04
Soil	S1-1	0-5	128	4	159	5	0.81	0.09	0.75	0.16
		5-10	<N.D.>		11	1	<N.A.>	0.04	0.71	0.25
		10-15	<N.D.>		8	0.5	<N.A.>	0.07	0.82	0.11
	S1-2	0-5	330	30	370	30	0.89	0.04	0.71	0.25
		5-10	<N.D.>		35	3	<N.A.>	0.05	0.58	0.37
		10-15	390	30	426	40	0.92	0.01	0.79	0.20

Radioactivity was corrected at released day, March 15, 2011. N.D. and N.A. show Not Detected and Not Available, respectively. Calculated detection limit is 4.5 Bq/kg and 5.2 Bq/kg for ^{134}Cs and ^{137}Cs, respectively.

Table III-3.2. Activity concentration of ^{134}Cs and ^{137}Cs on sand fraction and silt and clay fraction of lake sediment and soil

Sample		Deepness (cm)	^{134}Cs				^{137}Cs			
			Sand		Silt and Clay		Sand		Silt and Clay	
			2 mm – 70 µm		< 70 µm		2 mm – 70 µm		< 70 µm	
			Bq/kg	error	Bq/kg	error	Bq/kg	error	Bq/kg	error
Lake Sediment	L1-1	0-5	19	1	190	20	81	6	1880	220
		5-10	<N.D.>		81	7	16	1	440	50
		10-15	<N.D.>		42	4	26	2	660	80
	L1-2	0-5	23	2	56	5	86	7	700	70
		5-10	<N.D.>		<N.D.>		14	1	100	10
		10-15	<N.D.>		<N.D.>		37	4	110	10
	L2-1	0-5	15	1	20	1	100	10	250	20
		5-10	18	1	31	2	91	6	330	30
		10-15	<N.D.>		<N.D.>		12	1	73	8
	L2-2	0-5	27	2	<N.D.>		150	10	400	40
		5-10	29	1	44	5	190	10	700	60
		10-15	12	1	11	1	60	4	160	10
	L3-1	0-5	210	10	1460	60	1110	30	19730	850
		5-10	270	20	1680	70	1450	40	21060	890
		10-15	90	5	410	20	1020	40	6650	300
	L3-2	0-5	<N.D.>		<N.D.>		50	6	1450	180
		5-10	<N.D.>		<N.D.>		13	2	130	20
		10-15	<N.D.>		<N.D.>		6.8	0.9	90	10
Soil	S1-1	0-5	18	2	39	3	120	10	530	50
		5-10	<N.D.>		<N.D.>		10.1	0.8	37	4
		10-15	<N.D.>		<N.D.>		<N.D.>		60	7
	S1-2	0-5	84	7	130	10	820	70	1760	180
		5-10	7	1	15	2	86	8	66	7
		10-15	96	4	160	10	860	70	2370	260

Radioactivity was corrected at sampling day, August 8, 2016. N.D shows Not Detected. Sample L1-3 is not measured due to its low bulk concentration of radioactive cesium. Calculated detection limit is 3.8 Bq/kg and 5 Bq/kg for ^{134}Cs and ^{137}Cs, respectively.

III-4. Conclusions

The ^{134}Cs and ^{137}Cs were detected in all sediment of shallow area of lake, in which ratio of ^{134}Cs and ^{137}Cs decay corrected to the released day March 15, 2011 is about 1.

The depth profile of deposition density in sediment of shallow area of lake was a suitable information for indirect deposition process investigation. By assuming higher contribution of ^{134}Cs and ^{137}Cs derived from catchment, the depth profile of shallow lake sediment showed that the indirect deposition of ^{134}Cs and ^{137}Cs in sloped area was faster than in flat area. The indirect deposition process in flat area was probably more influenced by sediment flowed from river, whereas in sloped area it was probably more relied on erosion process during rain fall.

The silt and clay fraction holds dominantly the ^{134}Cs and ^{137}Cs than other fractions. The highest activity concentration on silt and clay fraction was always found at the peak layer. It probably shows that the silt and clay fraction was a medium of ^{134}Cs and ^{137}Cs indirect deposition into lake.

III-5. References

1 IAEA, FUKUSHIMA DAIICHI Accid. Tech. Vol. 1, 2015

2 Hayashi S., Global Environmental Research , 2016, 45–52.He Q, Walling DE, Owens PN, Chem Geol, 1996, 129:115–131. doi: 10.1016/0009-2541(95)00149-2

3 He Q., Walling D. E., Owens P. N., Chemical Geology, 1996, 129:115–131. doi: 10.1016/0009-2541(95)00149-2

4 Kitamura A., Yamaguchi M., Kurikami H. et al., Anthropocene, 2014, 5:22–31. doi: 10.1016/j.ancene.2014.07.001.

5 Putyrskaya V., Klemt E., Röllin S., Journal Environmental Radioactivity, 2009, 100:35–48. doi: 10.1016/j.jenvrad.2008.10.005.

6 Ochiai S., Nagao S., Yamamoto M., et al., Applied Radiation and Isotopes, 2013, 81:366–370. doi: 10.1016/j.apradiso.2013.03.073.

7 Campbell B. L. , Radioisotope Sediment Studies, 1983, 7–29.

8 Ligero R. A., Casas-Ruiz M., Barrera M. et al., Applied Radiation and Isotopes, 2010, 68:1602–1609. doi: 10.1016/j.apradiso.2010.02.010

9 Satoh Y., Sagisaka H., Japan Journal of Limnology, 1997, 58:359–372.

10 Yoshimura K., Onda Y., Fukushima T., Scienctific Report, 2014, 4:4514. doi: 10.1038/srep04514

11 Aoi Y., Fukushi K., Itono T., et al., Journal of Mineral and Petroleum Science, 2013, 109:23–27. doi: 10.2465/jmps.130620c.

12 Bostick B. C., Vairavamurthy M. A., Karthikeyan K. G., Chorover J., Environmental Science and Technology, 2002, 36:2670–2676. doi: 10.1021/es0156892

13 Sato K, Fujimoto K, Dai W, Hunger M., Journal Physical Chemistry C., 2013, 117:14075–14080. doi: 10.1021/jp403899w.

Chapter IV

Factors affecting ^{137}Cs migration from sloped forest catchment[1,2]

---

[1] Investigation of radiocesium migration from land to waterbody using radiocesium distribution and soil to sediment ratio: A case of the steep sloped catchment area of Ogi reservoir, Kawauchi Village, Fukushima

T. Basuki, W. C. Bekelesi, M. Tsujimoto, S. Nakashima, *Radiation Safety Management*, 19, (2020) 23-34. DOI 10.12950/rsm.190924

[2] Examination of Cs tolerant bacteria interaction with Cs^+ in aqueous solution and soil by using ^{137}Cs tracer

T. Basuki, K. Inada, S. Nakashima, *AIP-CP*, accepted (2020).

IV-1. Introduction

The Fukushima Daiichi Nuclear Power Plant (FDNPP) accident that occurred on March 15, 2011, caused a substantial amount of radioactive materials released to the environment. Among the radioactive materials released to the environment, radiocesium (^{134}Cs and ^{137}Cs) beside radioiodine (^{131}I) is the most major released volatile radionuclide having a direct impact to land contamination.1) The longer ^{137}Cs half-life (30.2 years) in comparison to ^{134}Cs (2.06 years) and ^{131}I (8 days) has made the ^{137}Cs as the main radionuclide of interest to be studied.

The distribution and migration of FDNPP accident-derived radiocesium in terrestrial environment over time have been widely investigated. The understanding of radiocesium migration behavior is key to the assessment of the long-term radiation hazard risk and its countermeasures. The soil-water body migration from forest catchment is the main feature in Fukushima because the forest area covers more than 60% of the contaminated zone and has higher radiocesium inventory in comparison to the other land use. 2, 3) Previous studies looked at the importance of elevation and slope aspects on radioactive materials migration in catchment over several years following the accident. 4-8) However, the more empirical finding regarding factors that influence the migration of radiocesium from catchment to water body is still needed.

Biological factor, especially soil microorganism, also might play an important role in radiocesium migration from the soil. The enhancement of Cs desorption from illite by bacteria exudate (*Bacillus* sp., *Ralstonia* sp. and *Enterobacter* sp.) was reported.9) The enhancement of Cs desorption was due to the mineral biological weathering process. It was reported that the interlayer expansion of vermiculite is due to mineral biological weathering. 10) The Cs leaching from fly ash by using acidophilic bacteria was also examined. 11) However, there are very few previous studies on Cs desorption from soil by bacteria, which is very important for understanding Cs migration in the environment and for bioremediation purposes.

In this chapter, we examined the ^{137}Cs distributions for investigating the radiocesium migration. We discussed the high radiocesium retention of the steep forest zone catchment by considering the physicochemical property of the surface soil.

Furthermore, we selected and isolated the high Cs tolerant soil bacteria and further examined the interaction between the isolated soil bacteria and Cs in aqueous solution and soil. The selected bacteria tolerance level, Cs absorption capacity from the solution and Cs desorption enhancement from soil were studied. It was expected to provide a comprehensive knowledge of isolated bacteria interaction with Cs in the environment, which might be important for understanding Cs mobility in the environment and for Cs bioremediation.

IV-2. Sampling and Experimental method

IV-2.1. Air dose rate measurement, sampling and sample measurement

The air dose rate measurement and soil sediment sampling were conducted in sloped catchment of Ogi Reservoir, Kawauchi Village, Fukushima on March 15-16, 2018. The measurement and sampling site in the catchment were divided into area 1 and area 2 (forest area) and area 3 (transition zone, no vegetation) along the slope, see Figure IV-2.1. The air dose rate was measured by survey meter with NaI detector (ALOKA MYRATE PDR-111) 1 m above the ground. The soil sample was collected by hand core sampler (25 cm long tube, 19.6 cm^2 area) and the sediment sample was collected by gravity core sampler (6.5 cm diameter and 60 cm long tube, geographic position and elevation of measurement and sampling sites were recorded using GPS locator (Garmin, Oregon 650TCJ).

^{134}Cs and ^{137}Cs in soil and sediment samples were measured by Gamma spectrometer with HP Ge detector (GEM 30-70, ORTEC).

Physicochemical properties of soil samples were analyzed, including soil density, pH, size fraction, organic matter content, major cation concentration, cation exchange capacity (CEC) and base saturation.

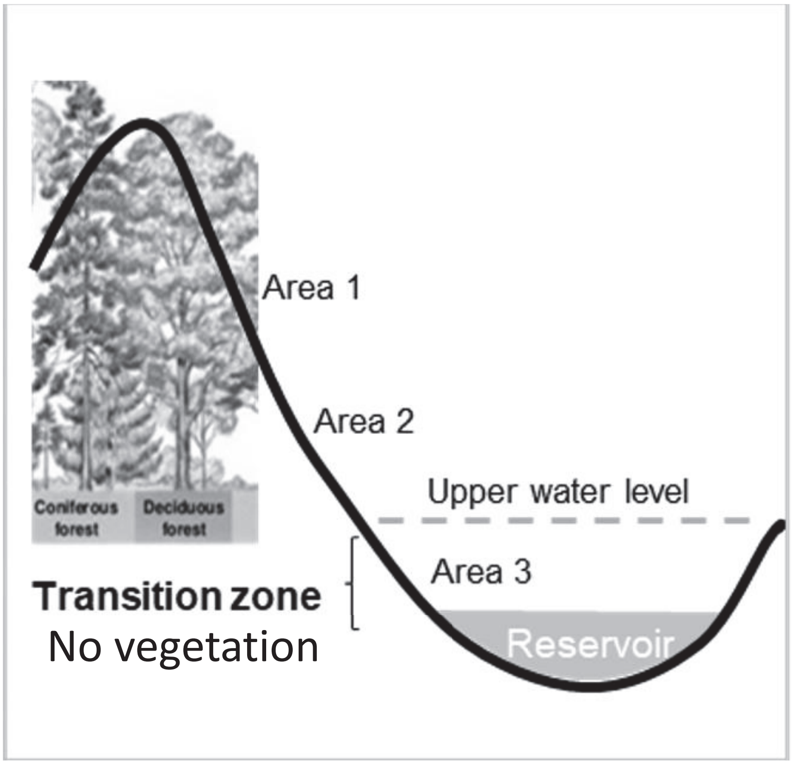

Figure IV-2.1. Illustration of the sampling area in the catchment.

IV-2.2. Cs sorption by soil bacteria experiment

The source of bacteria is from the soil of Higashi-Hiroshima campus, Hiroshima University. 3 g of soil was mixed with 27 ml distilled water and thereto 2.7 g glass beads were added and whirled at maximum speed for about 1 minute to make soil slurry. Series of dilution ($10^0 \sim 10^{-4}$) was conducted and the diluted samples were inoculated to liquid medium to make bacteria seed culture.

The seed culture was inoculated in the liquid medium and solid media containing CsCl 10 mM, 50 mM and 0 mM (as control). The liquid culture was conducted for 5 days at 120 rpm, 25°C and solid culture was conducted for 3 days at 25°C. Bacteria sample from 50 mM CsCl liquid culture was further inoculated to new medium containing 50 mM CsCl and repeated 3 times for screening the Cs high tolerant bacteria. The growth of bacteria in liquid medium was measured by 600 nm absorbance (CO7500 colorimeter, WPA color wave). The selected bacteria sample was grown on solid media, 10 colonies that grew on the plate were randomly picked up and transferred to new media for identification.

The content of the growth medium was 0.5% tryptone, 0.25% yeast extract, and 0.1% d-glucose. In the case of solid media, 1.5% of agar was added to the growth media.

Isolated bacteria were grown in the liquid medium for 24 h with wide range of CsCl concentration (0.01, 0.1, 1, 10, 50, 100, 200, 300, 400 mM). Small amount of ^{137}Cs was added to the medium with known CsCl to ^{137}Cs concentration ratio. The cell solution sample (5 ml) was collected after 24 h culture, washed with distilled water 4 times to remove the Cs loosely adsorbed to bacteria, centrifugated in 3000 rpm and dried in the oven (105°C) for 12 h. The dried cell was measured using gamma spectrometry with low background HP Ge detector (GEM 30-70, ORTEC) to determine the ^{137}Cs activity concentration.

The CsCl concentration was calculated by considering the CsCl to ^{137}Cs concentration ratio, as shown in equation (1).

$$[CsCl] = A \times r \tag{1}$$

where [*CsCl*] CsCl concentration (mol/g), *A* activity concentration of ^{137}Cs in dried sample (Bq/g) and *r* CsCl to ^{137}Cs ratio (mol/Bq).

Furthermore, the dried cell that grew under 100 mM and 300 mM CsCl, 100 mM KCl and 0 mM (control) were analyzed by FE-SEM. The cell of 24 h culture was harvested, washed 3 times with distilled water, centrifugated in 3000 rpm, fixed by Glutaraldehyde 2.5% and dehydrated by alcohol series (10, 30, 50, 70, 90, 100% ethanol). The dehydrated samples were dried overnight in a desiccator.

IV-2.3. Cs desorption from soil experiment

Soil was dried at room temperature and further dried in oven (105°C). The soil was sieved by electric rotating sieve set (SKH-01, AS ONE) with some mesh size ($x > 2$ mm, 2 mm $> x >$ 850 μm, 850 μm $> x >$ 250 μm, 250 μm $> x >$ 75 μm and $x <$ 75 μm). The soil fraction < 75 μm subjected as silt and clay was used in the experiment. The silt and clay fraction is the soil fraction that has the highest Cs concentration than other soil fraction [13]. The soil was washed 3 times with distilled water (1/20; w/v), to remove the salts and dried in the oven at 105°C for 12 hours. ^{137}Cs was added to the soil, by mixing 30 ml ^{137}Cs solution (~400 Bq/ml), 10 ml distilled water and 10 g soil, whirled with maximum speed for 5 minutes and further shaken for equilibration (12 h). The mixture was centrifugated in 4000 rpm and the precipitate was dried in oven (105°C). The dried soil was measured using gamma spectrometer to measure the ^{137}Cs activity concentration in the soil. The measured ^{137}Cs value in the soil was 3,400 ±100 Bq/g.

Bacteria sample was prepared by growing 10 µl bacteria isolate solution in flask containing 100 ml liquid medium (2 flasks) for 24 h. The bacteria sample was harvested, washed 2 times with distilled water and concentrated to be 20 ml isolated bacteria enriched solution.

Cs leaching from soil experiment was comprised of biotreatment batch, acid treatment batch, and control. 0.5 g soil <75 µm was added to each 40 ml broth batch and control. In biotreatment batch, about 5 ml enriched isolated bacteria solution was added, pH was adjusted to be 7. At acid treatment, 4 M H_2SO_4 was added to adjust the pH of broth to be 2. Furthermore, it was shaken in bio shaker, 120 rpm, 25°C. The sample was collected at interval 0.5, 1, 2, 3, 9, 15 h for measuring ^{137}Cs released to the solution. The collected sample was centrifugated in 4000 rpm for 3 minutes, the supernatant was filtered by syringe filter set, 0.45 µm pore (Minisart RC 15, Sartorius stedim). The ^{137}Cs concentration in solution was measured by gamma ray measurement with NaI (Tl) well-type scintillation detector (Auto well gamma system, ARC-380 CL, ALOKA). The pH of solution was measured using pH meter (F-55, HORIBA).

IV-2.4. DNA preparation and 16S rDNA partial sequence of isolated bacteria

The total DNA of microorganisms was prepared with ZR Fungal/Bacterial DNA MiniPrep^{TM} kit (ZYMO RESEARCH) according to the instruction manual.

A fragment of the 16S rDNA partial gene was amplified by PCR using 357F primer (5'-CCT ACG GGA GGC AGC AG - 3') and 907rC (5'- CCG TCA ATT CCT TTR AGT TT - 3'). 12) Amplification of the 16S rDNA partial gene was performed with AmpliTaq^{R} DNA polymerase, LD (Life Science Technologies) under the following conditions: 2 min at 95 °C to denature the DNA, and touchdown cycle was performed (5 cycles of denaturation at 94 °C for 30 sec, annealing at 65 °C for 30 sec, and extension at 72 °C for 1 min) and annealing temperature decreased by 2 °C every 5 cycles until the temperature reached 57 °C. And then 30 cycles consist of 30 sec at 95 °C, 30sec of 60 °C, and 1min at 72 °C and then 1 cycle consists of 5 min at 72 °C. The amplified PCR products were separated from unreacted primers with agarose gel electrophoresis and extracted with PCR clean-up Gel extraction kit (NucleoSpin^R Extract II) (MACHEREY- NAGEL) according to its user manual.

The 16S rDNA partial gene was sequenced by using 310 genetic analyzer, ABI PRISM. The 16S rDNA partial gene sequence against the 16S ribosomal DNA sequences (Bacteria and Archaea) database was used to determine to which bacteria the isolates were closely related. 13)

IV-3. Results and Discussions

IV-3.1. Physical and chemical factors

IV-3.1.a. Type of ^{137}Cs initial deposition and land use in ^{137}Cs distribution

The ^{134}Cs and ^{137}Cs concentrations in the soil of catchment area show a very strong relationship, with its ratio of sampling day (March, 2018) about 0.11 and its ratio of decay corrected to released day (March 15, 2011) about 0.94, see Figure IV-3.1. The value of ^{134}Cs to ^{137}Cs ratio decay corrected to released time shows that the radiocesium was derived from FDNPP accident and more particular was mostly from the reactor unit 1. [14)]

The data of air dose rate along the gradient elevation are presented in Figure IV-3.2. (a). The air dose rate was ranged from 0.59±0.12 to 1.6±0.07 $\mu Sv\cdot h^{-1}$. Higher air dose rate was found in Area 1 and Area 2 which are the higher elevation area and mixed forest area in comparison to Area 3 (lower elevation and no forest or transition zone).

The relationship between the air dose rate and ^{137}Cs inventory along the gradient elevation was shown in Figure IV-3.2.b. It shows that the air dose rate increased with the increase of ^{137}Cs inventory in the soil. It further shows that ^{137}Cs was main source of radiation in the study area.

The results obtained in Figure VI-3.2. showed that the air dose rate and ^{137}Cs inventory were to some extent heterogeneous. The air dose rate and ^{137}Cs inventory in the higher elevation area (area 1) were higher than lower elevation area (area 2 and area 3). Moreover, in the lower elevation area (area 3, transition area), there showed a very large decrease of the air dose rate compared to the higher areas (area 1, area 2).

The heterogeneous distribution with the tendency of higher air dose rate and ^{137}Cs inventory in higher elevation area probably occurred by dry initial deposition process of radionuclides from the atmosphere. It has been discussed previously that the atmospheric wet initial deposition resulted in more homogenous distribution than the dry initial deposition.4) Kawauchi area as the present study research area had received radioactive contamination through the dry initial deposition for about 60~70%.15) The higher radioactive contamination found in higher elevation area was in line with some results of a previous research that showed the elevation dependence of the radioactive contamination in dry deposition area, especially in the slope facing FDNPP.5)

The obtained finding of horizontal distribution is not in line with some previous researches which showed the increase of radioactive contamination along the decrease of elevation that probably corresponded to lateral indirect deposition or redistribution in sloped area.4,6,7) Some previous researches show more radiocesium accumulation in the middle and bottom of the slope7) and accumulation in the water body in steep sloped area.8) This difference is probably because of the difference in land use type and initial radiocesium deposition type that occurred among the study areas.

Moreover, the obtained results show that the horizontal distribution of air dose rate and ^{137}Cs inventory were more dependent on the land use type. The air dose rate was more homogenous in the forest zone (area 1 and area 2) across the steep slope and decreased sharply in the transition zone (area 3). It shows, even in the steep sloped area, the forest zone highly retained the radioactive contaminant in comparison to the transition zone. The same tendency of high radiocesium retention in the forest was shown in some previous researches. 2,16)

The vertical distributions of ^{137}Cs in soil and sediment are presented in Figure IV-3.3. In the case of soil catchment, the ^{137}Cs was accumulated in the upper layer of soil as an overall tendency. However, in more detail, the ^{137}Cs penetrated more in the soil of area 1 and area 2 (forest soil) in comparison to the transition zone (area 3). The data show that about 90% of deposited radiocesium in the case of transition zone was accumulated on 17±2 kg･m^{-2} soil at 0~2 cm layer (the less mass and thinner depth) in comparison to forest zone, 48±10 kg･m^{-2} soil (coniferous forest) and 26±6 kg･m^{-2} soil (deciduous forest) at 2~6 cm layer. Whereas, in the case of sediment, ^{137}Cs was accumulated in deeper layer. The surface layer of sediment contains less ^{137}Cs. About 90% of deposited ^{137}Cs was in between 100 and 200 kg･m^{-2} surface sediment or in between 10 and 30 cm physical depth.

The obtained vertical profile data show deeper accumulation of radiocesium in sloped forest zone than in the transition zone (Figure IV-3.3.). This finding was in line with the previous research that showed deeper radiocesium accumulation in the forest than other undisturbed areas such as uncultivated cropland and grassland. 17) Figure IV-3.3. also shows the very different depth profile of soil and sediment. The depth profile of soil probably showed the radiocesium inventory depletion that probably due to radiocesium migration and soil erosion. The sediment depth profile showed the radiocesium inventory accumulation along the time.

Deeper radiocesium accumulation in the sloped forest zone than transition zone was probably one of the factors that could inhibit horizontal migration of particulate radiocesium into water body, even in the very steep sloped area. Besides the bio-physical factor such as forest canopy protection, the deeper radiocesium accumulation in soil surface probably provided an indirect protection from horizontal migration through surface water runoff mediating particulate cesium migration. The deeper the accumulation of radiocesium on forest surface layer, the less reachable the radiocesium by surface water runoff.

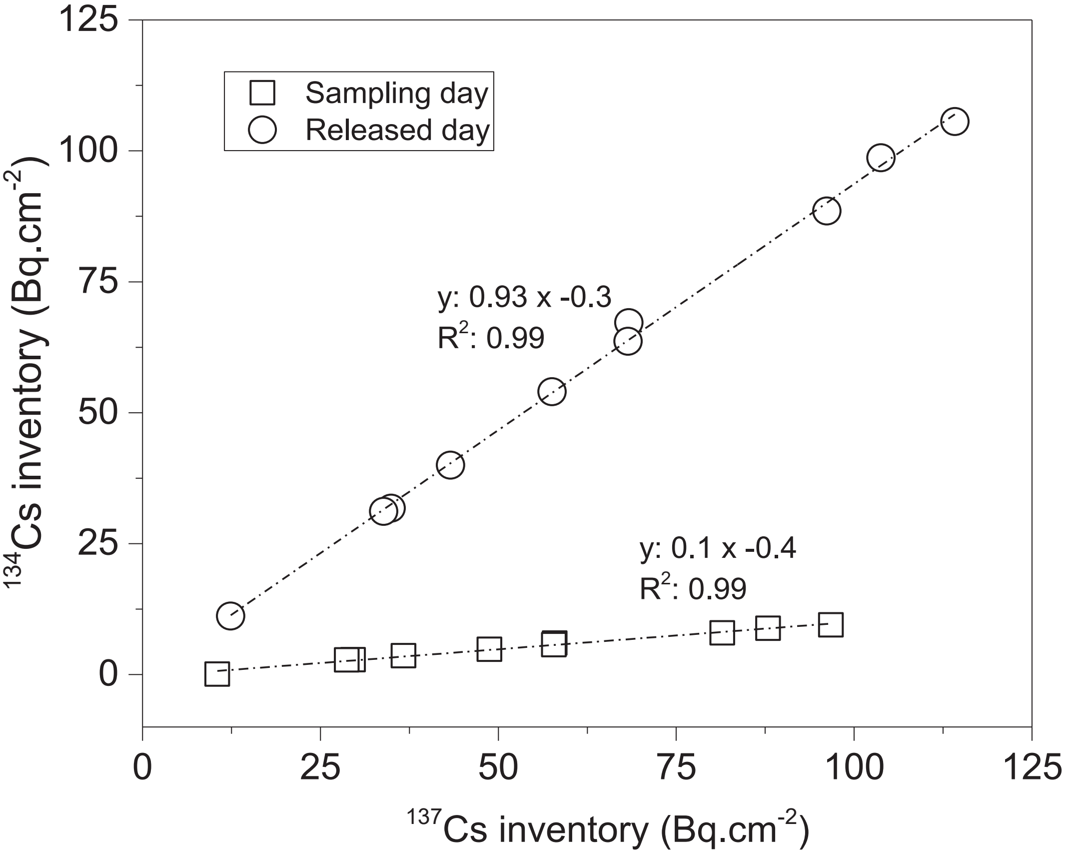

Figure IV-3.1. ^{137}Cs and ^{134}Cs inventory decay corrected at sampling and released day.

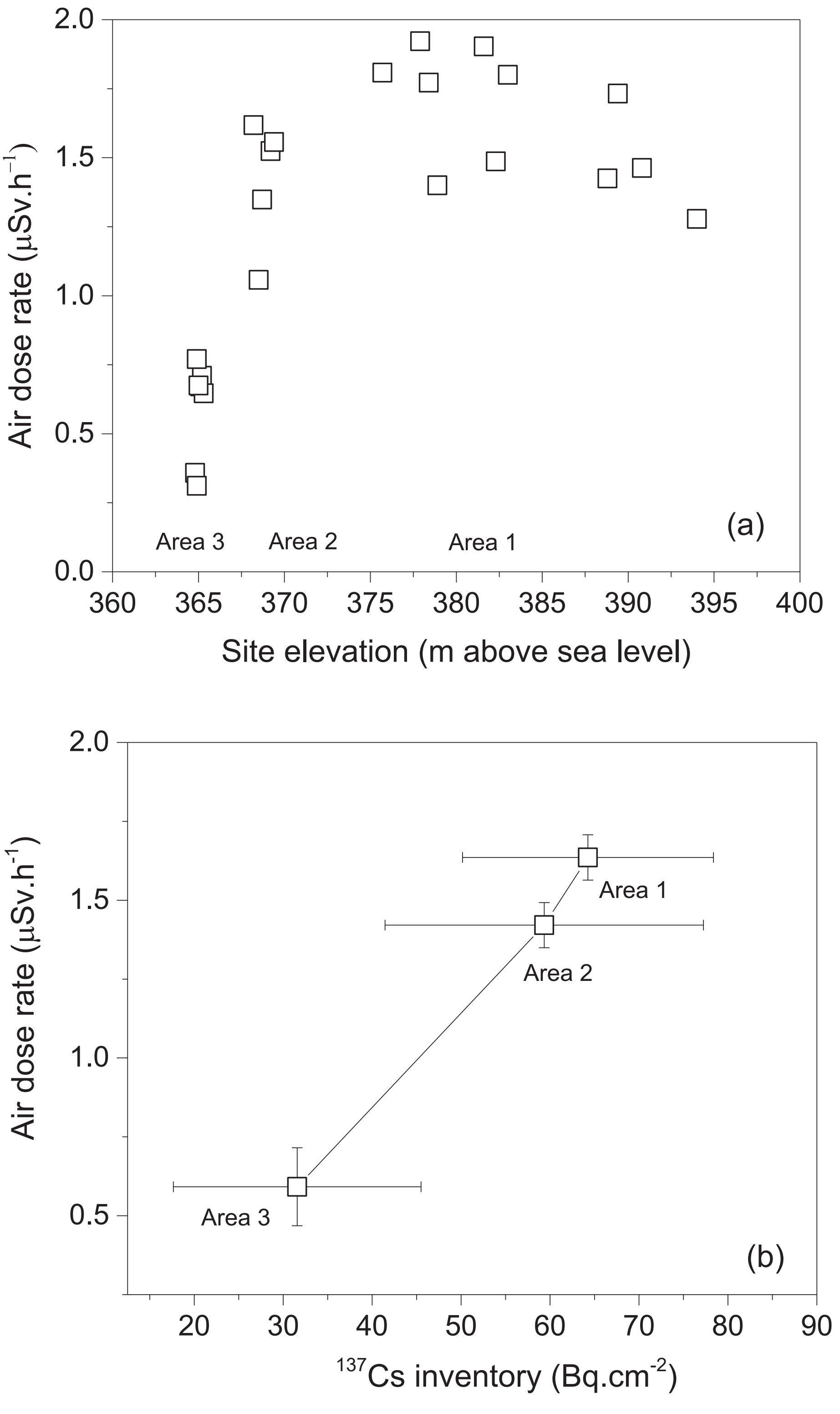

Fig IV-3.2. Air dose rate along site elevation (a), ^{137}Cs inventory and air dose rate of the slope catchment (b).

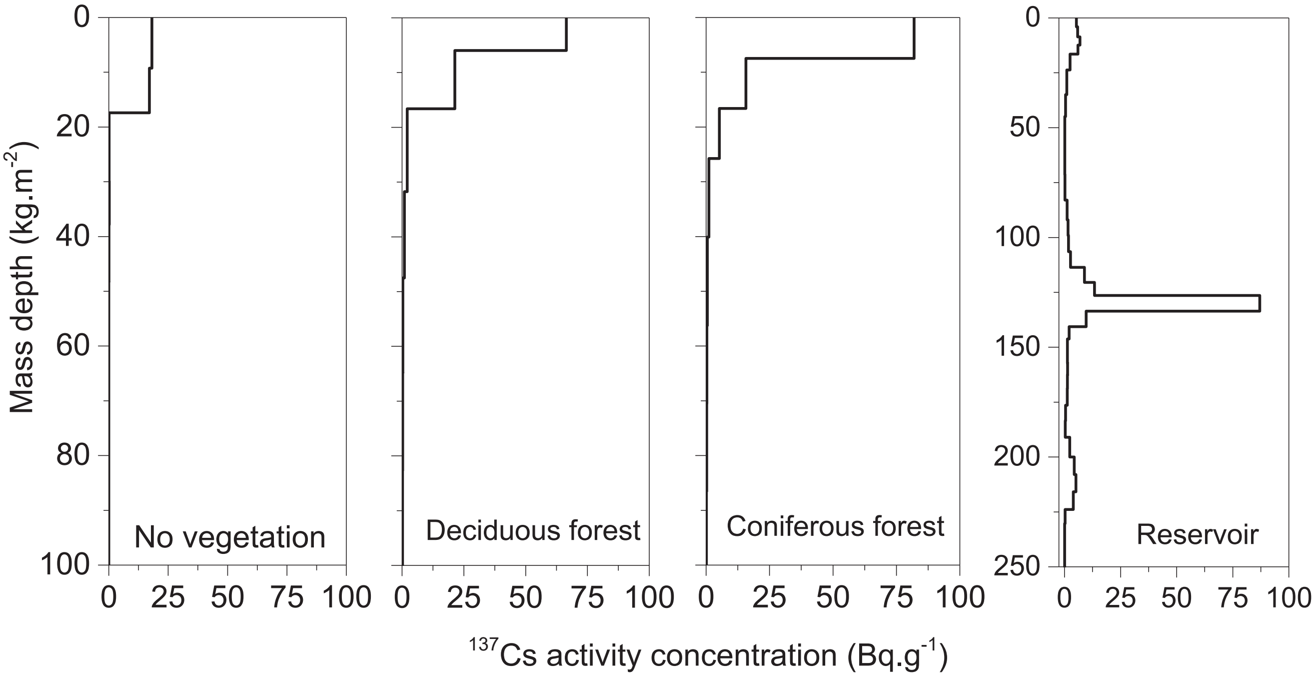

Figure IV-3.3. Vertical profile of ^{137}Cs concentration of soil catchment and reservoir sediment. Each increment equals to 1 cm and 2 cm depth for sediment and soil, respectively.

IV-3.1.b. Physicochemical property of the forest surface soil and the inhibition of radiocesium migration from the catchment

Table IV-3.1. summarizes the physicochemical properties of the soil samples of the present study area. The measured soil samples are in the surface layer of 0-2 cm depth. The value is a calculated mean value of samples and the error value is calculated based on the standard deviation.

The bulk density, excluding the particle size >2 mm, ranged from 0.30±0.10 to 0.46±0.10 g.cm^{-3}. Transition zone surface soil has a higher bulk density (0.46± 0.10%) than the forest zone surface soil, 0.30±0.10% (deciduous forest) and 0.37±0.20% (coniferous forest).

The soil pH of all land use was acidic, ranged from 4.3±0.1 to 4.7±0.1. The pH of the transition zone is relatively higher (4.7±0.1) than deciduous forest (4.6±0.3) and coniferous forest (4.3±0.1).

The CEC value of surface soil was relatively different between the transition zone 59±8 and forest zone, 54±16 (deciduous forest) and 99±23 (coniferous forest). However, the base saturation value of all samples was relatively low for all samples, ranged from 8.4±3.7 to 12±5 that means only about 6.0~12% was occupied by the major cation or there was still a large space of surface soil to hold additional cation.

Table IV-3.1. also shows a notable difference in organic matter content and soil fraction content <75µm between the transition zone and forest zone. The soil of active zone contains higher soil fraction <75µm (about 66±9%) and less organic matter (about 19±4%) than forest soil that contains soil fraction <75µm about 17~21% and organic matter about 26~48%.

Some physicochemical properties of surface soil such as bulk density, fine particle content, and organic matter content were probably the underlying factors that contributed to the radiocesium deeper accumulation in the forest zone. Table IV-3.1. shows the general tendency that the forest surface soil contained lower fine grain and bulk density and higher organic matter content than transition zone soil which probably promoted the ^{137}Cs penetration depth. Previous research showed the positive correlation between ^{137}Cs retention in 0-1 cm layer and bulk density and negative correlation between ^{137}Cs retention in 0-1 cm layer and organic carbon content in clay.17) The faster vertical migration of ^{137}Cs in the litter layer of forest floor within one year after accident was reported and the vertical migration becomes very slow once it reached mineral layer.11) However, previous research showed that ^{137}Cs retention in the litter layer of the forest floor can delay the radiocesium penetration onto soil.3)

Regarding the soil particle size dependence on radiocesium concentration, it has been widely known that finer particle size especially clay fraction can adsorb and fix the radiocesium strongly. 8, 18, 19) However, the high content of organic matter could inhibit the sorption of radiocesium by the clay material. 11) The decomposition of litter in the surface soil of forest zone forms mobile soluble organic matter complex compound with cation including ^{137}Cs.17)

Table IV-3.1. Physicochemical property of surface soil catchment (0-2 cm depth)

Area	Soil sample (*n*)	Bulk density ($g \cdot cm^{-3}$)	pH (H_2O)	OM fraction (%)	Size fraction <75μm (%)	Exchangeable cation ($cmol \cdot kg^{-1}$)				CEC ($cmol \cdot kg^{-1}$)	Base saturation (%)
						Na^+	K^+	Mg^{2+}	Ca^{2+}		
Area 1 (Forest)	4	0.30 ± 0.10	4.3 ± 0.1	48 ± 18	17 ± 7	0.20 ± 0.04	0.51 ± 0.18	0.69 ± 0.28	6.9 ± 3.1	99 ± 23	8.4 ± 3.7
Area 2 (Forest)	3	0.37 ± 0.20	4.6 ± 0.3	26 ± 11	21 ± 3	0.11 ± 0.02	0.38 ± 0.16	0.47 ± 0.19	6.3 ± 2.5	54 ± 16	12 ± 5
Area 3 (No vegetation)	3	0.46 ± 0.10	4.7 ± 0.1	19 ± 4	66 ± 9	0.23 ± 0.15	0.28 ± 0.03	0.35 ± 0.04	4.5 ± 0.4	59 ± 8	9.1 ± 1.4

IV-3.2. Biological factors

IV-3.2.a. Cs toxicity toward soil bacteria and Cs tolerant bacteria

The Cs apparently showed the growth effect of soil bacteria, even at relatively low concentration, 10 mM CsCl, as shown in Fig IV-3.4 (a) and (b). The bacteria growth peak was delayed and lowered in the case of 10 mM and 50 mM CsCl, Fig IV-3.4 (a). Conversely, 50 mM KCl did not show bacteria growth inhibition effect as K is an essential element for the organism. It showed that the Cs is a toxic element. The toxicity of Cs^+ toward soil bacteria in general might be a result of either reduced influx or increased influx of K^+. 20, 21)

As a result of screening, the Cs high tolerant bacteria was successfully obtained which is named CsT-tb strain here and after. As a comparison, the bacteria that was cultured in broth without Cs^+ and with 50 mM K^+ supplement showed lower tolerance toward Cs^+, see Figure IV-3.5. Furthermore, the tolerance level toward Cs^+ of selected bacteria was shown up to 400 mM CsCl.

The high tolerance level of certain bacteria toward Cs^+ was probably due to the sequestration process of Cs^+ by vacuoles or change in the activity and/or specificity of Cs^+ transport system. 20) It was reported that the high tolerance level toward Cs^+ of *Flavobacterium sp.* was due to the ability to maintain the intracellular Cs^+ concentration by regulating the Cs^+ efflux. 22)

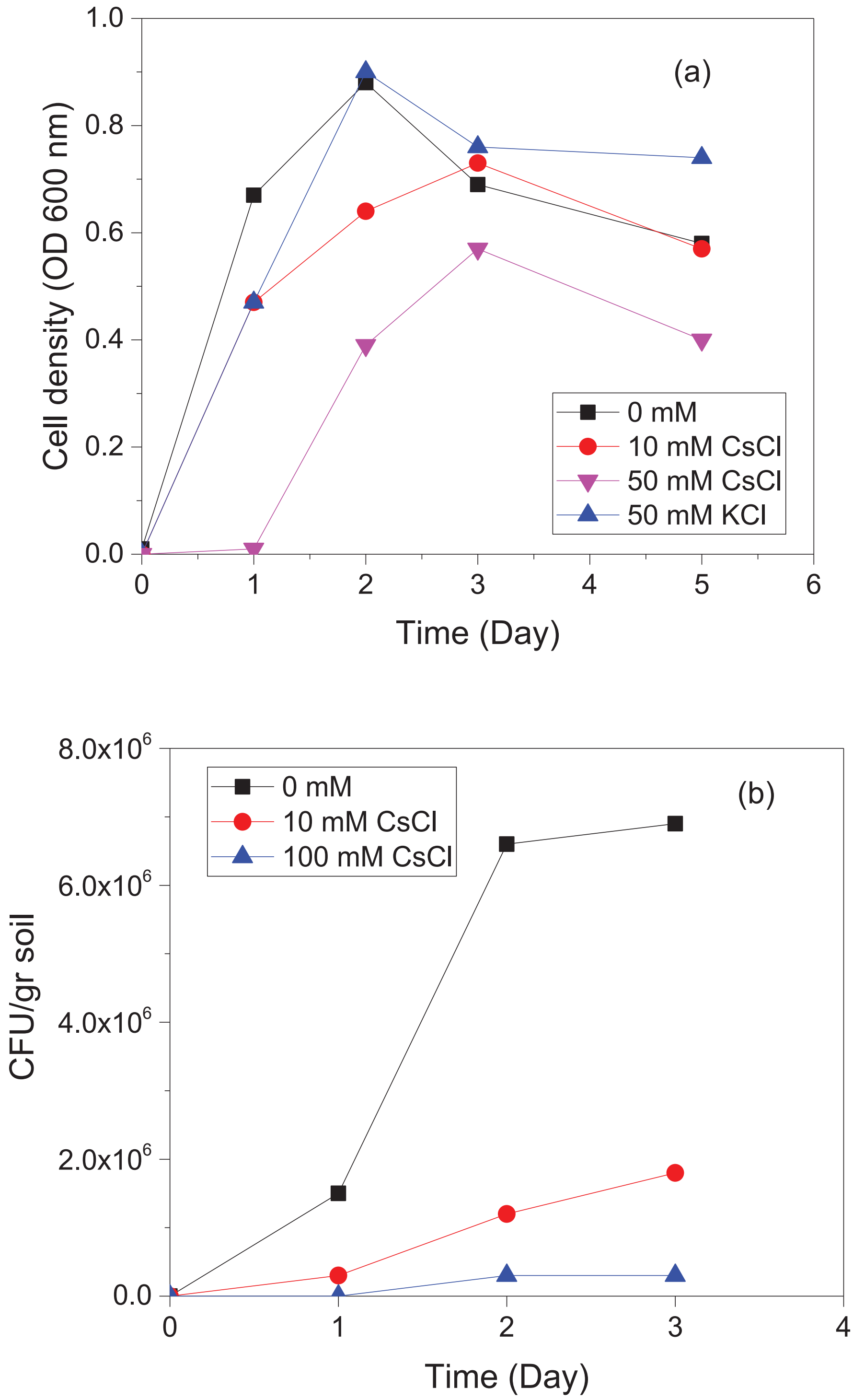

Figure IV-3.4. Cs toxicity toward soil bacteria grown at 25°C, pH 7, in liquid culture (a) and solid culture (b); with presence of CsCl.

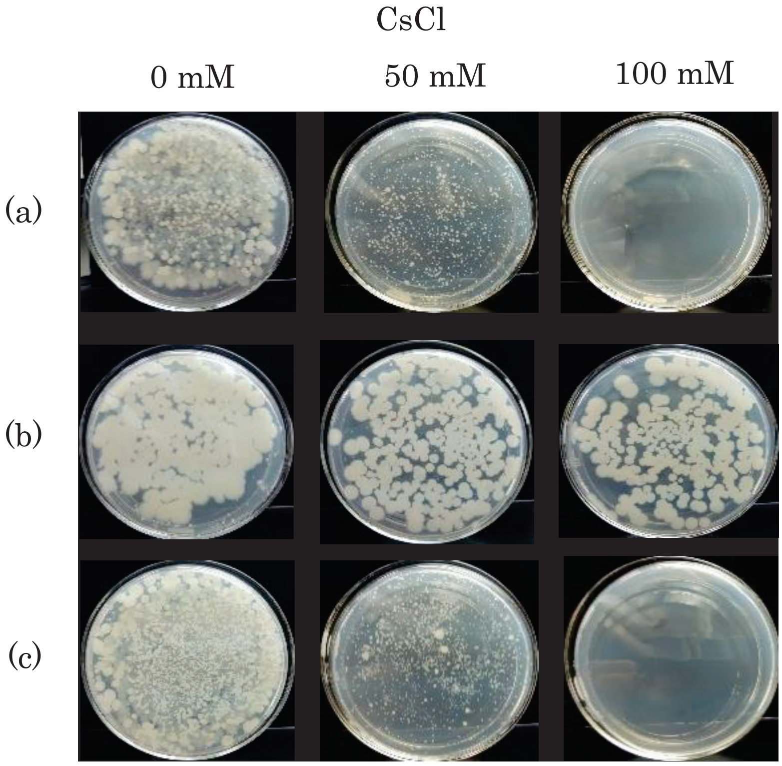

Figure IV-3.5. Cs$^+$ against bacteria; soil bacteria (a), selected bacteria that previously grew under 50 mM CsCl (b), bacteria that previously grew under 50 mM KCl (c).

IV-3.2.b Cs sorption by CsT-tb strain isolate

CsT-tb strain isolate has an ability to absorb Cs^+ depending on the Cs^+ initial concentration in the solution. The absorbed Cs^+ was increased with the increase of Cs^+ initial concentration in the solution, see Table IV-3.2. The similar tendency was also found in the case of Cs^+ absorption by *Saccharomyces cerevisiae.* 23) The intracellular monovalent cation absorption by bacteria depending on extracellular concentration was probably a passive diffusion phenomenon through the transportation channel located in the cell wall. 24) This process is mostly energy independent. So that it does not need the proton-motive force (PMF) or nucleoside triphosphates (NTPs) such as ATP and GDP to import the substrates. While, in general, monovalent cation flux through the cell membrane was against the concentration gradient, i.e., energy-dependent process. 20)

Furthermore, the maximum absorbed Cs^+ by CsT-tb strain was reached at 300 mM Cs^+ initial concentration in the solution. The absorbed Cs^+ was decreased sharply at Cs^+ initial concentration 400 mM. This Cs^+ absorption pattern probably can be explained from the growth curve of CsT-tb strain along the gradient Cs^+ initial concentration, see Figure IV-3.6. The Cs^+ initial concentration above 200 and 300 mM showed the lower growth peak of CsT-tb strain. Furthermore, 400 mM Cs^+ initial concentration apparently showed the CsT-tb strain growth effect that could mean 400 mM Cs^+ was the Cs^+ toxic level for CsT-tb strain. The FE-SEM image showed the cell wall deformation of CsT-tb strain that was cultured with the addition of 300 mM Cs^+, see Figure IV-3.7. It probably showed that the Cs^+ in the environment has surpassed the tolerable level.

Cs^+ absorption by CsT-tb strain was influenced by the presence of K^+ in solution, see Table IV-3.2. In the case of lower initial concentration ($\leq$ 10 mM), the presence of K^+ increased the Cs^+ absorption by CsT-tb. This finding probably showed a more active absorption that was triggered by the presence of small amount of K^+ in the environment, as the K^+ is essential for the bacteria growth. However, in the case of higher initial concentration (≥ 50 mM), the presence of K^+ could decrease the Cs^+ absorption by CsT-tb strain. This finding was in line with the idea that Cs^+ absorption by bacteria was through the same K^+ transport pathway considering that the physicochemical properties of Cs^+ and K^+ resemble.20,25,26) Therefore, the coexistence of high concentration of Cs^+ and K^+ in the solution would alternate each other in passing through the K^+ transport pathway.

In comparison to the other bacteria reported by previous reports, Cs^+ sorption by CsT-tb strain was relatively low, except *Arthrobacter sp.* strain KMSZP6, see Table IV-3.3. The tendency was the higher tolerance level of bacteria toward Cs^+ which would have the lower Cs^+ absorption capacity. It might be relevant with the notion that the high tolerance level of bacteria toward Cs^+ was due to the ability of the bacteria to maintain the Cs^+ intracellular concentration.

Table IV-3.2. Effect of Cs^+ initial concentration and presence of K^+ on Cs^+ absorption by CsT-tb strain

Initial concentration in solution (mM)	CsCl		CsCl and KCl	
	Absorbed Cs (μmol/g)	err (±)	Absorbed Cs (μmol/g)	err (±)
0.01	0.010	0.001	*n.a.*	
0.1	0.190	0.004	2.5	0.38
1	1.5	0.17	14	0.60
10	28	2.3	70	2.9
50	110	10	90	20
100	310	10	200	10
200	1,140	30	*n.a.*	
300	1,950	80	*n.a.*	
400	990	20	*n.a.*	

na: not available

Table IV-3.3. Cs^+ tolerance level and sorption of other bacteria

Bacteria	Tolerance level toward Cs^+ (mM)	Cs^+ absoprtion		References
		Cs^+ initial concentration in solution (mM)	Absorbed Cs (μmol/g) cell dry weight	
Rhodococcus sp. strain CS402	*n.a.*	0.01	98.3	Tomioka N. et al., 1994
		0.1	395	
		1	348	
Rhodococcus erythrophilis		0.01	127	
		0.1	615	
		1	533	
Flavobacterium chungbukense	>200	50	220	Kato S. et al., 2016
Flavobacterium sp. strain 200Cs-4	50	50	470	
Arthrobacter sp. strain KMSZP6	400	75	75	Swer P. B. et al., 2016

na: not available

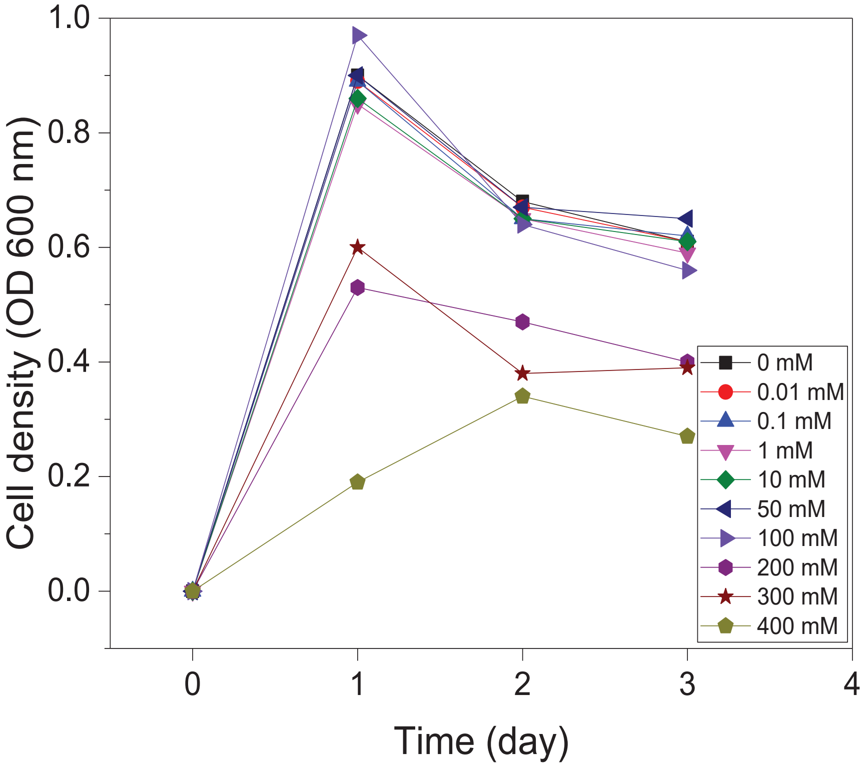

Figure IV-3.6. CsT-tb strain growth curve from low to high Cs concentration, at 25°C, pH 7.

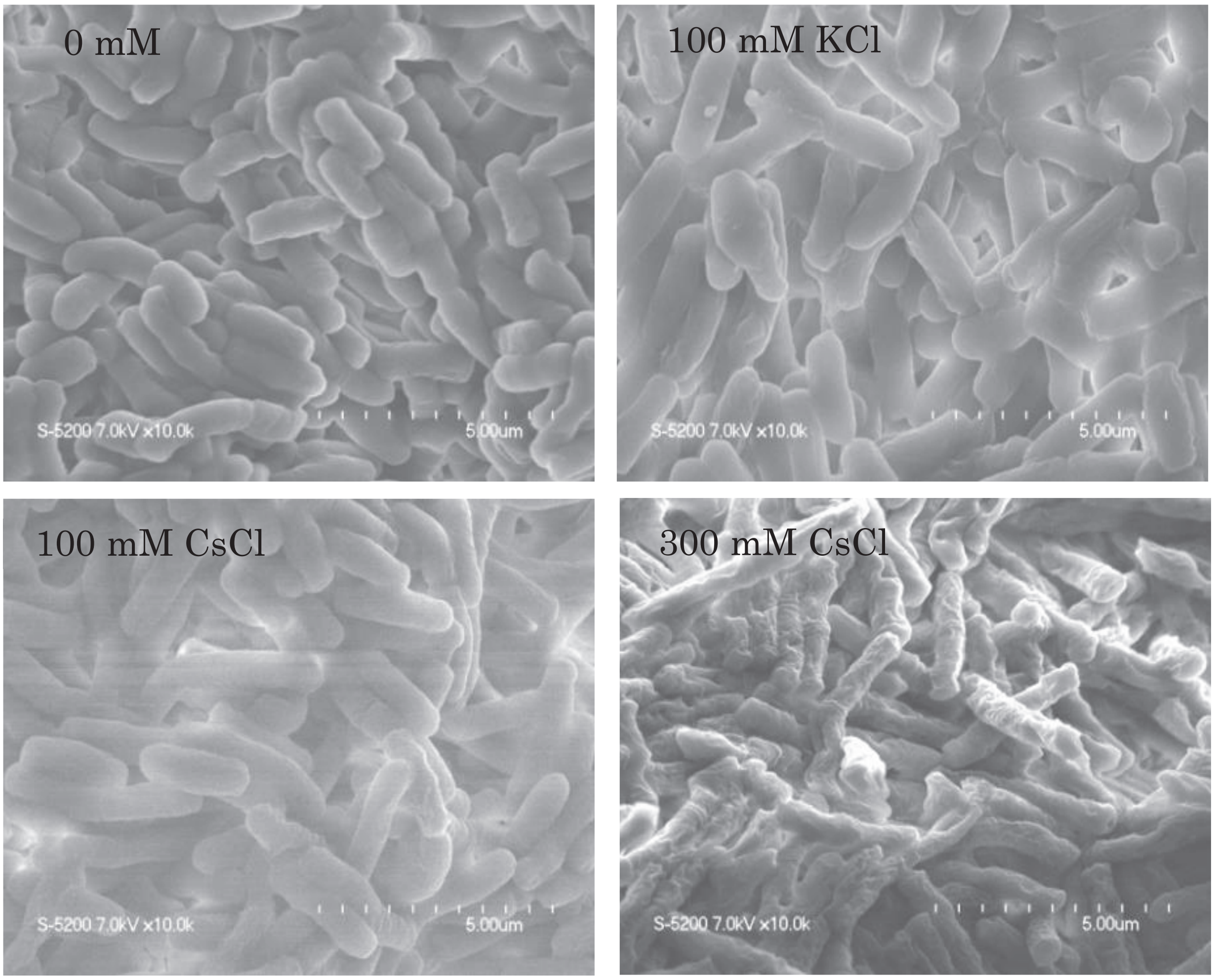

Figure IV-3.7. FE-SEM image of CsT-tb strain that grew under 0 mM, 100 and 300 mM CsCl and 100 mM KCl.

IV-3.2.c. Cs desorption enhancement from silt and clay fraction of soil by CsT-tb strain.

The influence of biotreatment was analyzed by adding CsT-tb strain solution to the broth containing Cs adsorbed to soil. About 5% additional Cs removal from the soil <75 μm was shown by CsT-tb strain treatment, which has a comparable Cs removal with H_2SO_4 treatment, see Figure III-3.8. (a). The pH of the solution was slightly increased during the experiment, see Figure III-3.8. (b).

The enhancement of Cs^+ desorption by CsT-tb strain bacteria was in line with the previous research that reported the Cs^+ desorption enhancement from illite by *Bacillus* sp. exudate solution treatment, about 4% enhancement.9) The bacteria exudates could promote the Cs^+ desorption by enhancing the mineral weathering by which the particle size decreases. The other studies reported the interlayer expansion of vermiculite by biological weathering process.10,27) Cs^+ desorption enhancement from fly ash by acidophilic bacteria was also reported.11) The Cs removal by bacteria showed its time dependence in which the maximum Cs removal was reached after 9 h.

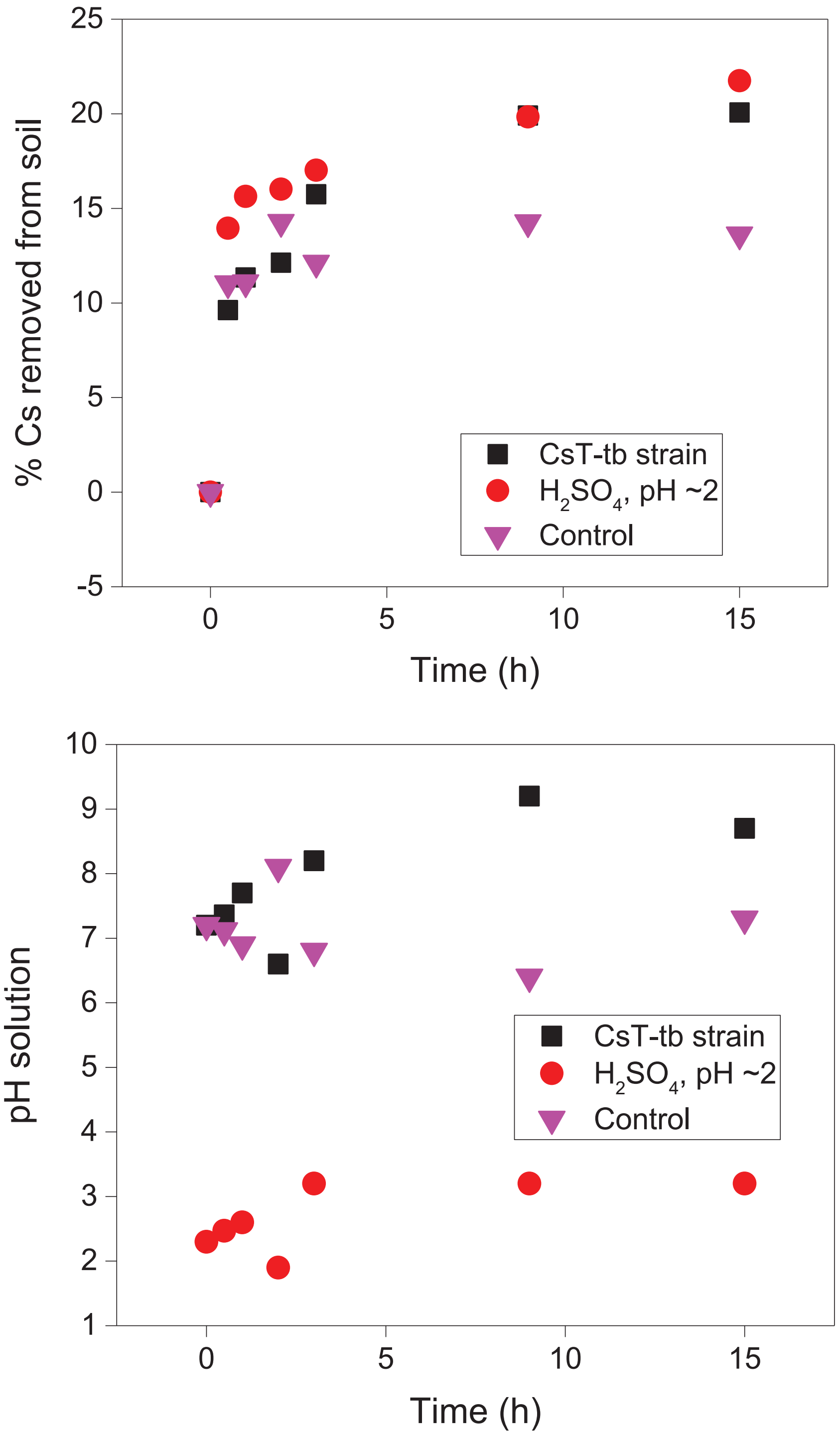

Figure IV-3.8. Cs desorption from the soil in the presence of CsT-tb strain and H_2SO_4, pH change during the desorption experiment.

IV-3.2.d. Identification of strain CsT-tb

From the phylogenetic tree based on 16S rDNA partial gene sequence of CsT-tb strain, the CsT-tb strain was closely related to *Bacillus* sp, see Fig IV.9. It was also confirmed from the FE-SEM image which shows the CsT-tb strain has rods shaped, see Figure III-3.7.

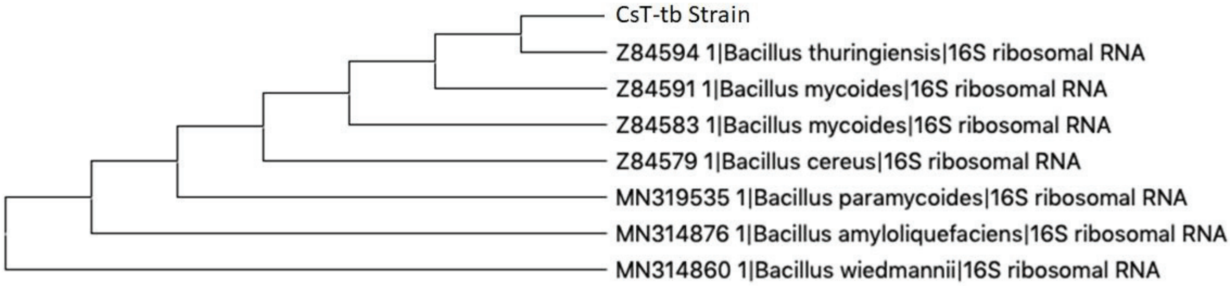

Figure IV-3.9. Phylogenetic tree based on 16S rDNA partial gene sequence of CsT-tb strain.

IV-4. Conclusions

We showed the horizontal distribution of air dose rate and radiocesium in the steep sloped catchment that was relatively heterogeneous and found a higher radiocesium inventory in higher elevation and forest area. This probably corresponded to the atmospheric dry initial deposition-derived radiocesium and the high retention of ^{137}Cs in the steep sloped forest area. The migration of ^{137}Cs from catchment to reservoir was probably contributed more from the transition zone. The sediment vertical profile showed the accumulation of ^{137}Cs in the deeper layer of sediment. The physicochemical property of the forest surface soil could be a possible factor of high retention of radioactive contaminant in the steep sloped forest zone.

The soil bacteria interaction with Cs^+ in aqueous solution and soil was examined. The growth of soil bacteria was affected by high concentration of Cs^+ confirming the toxicity of Cs. CsT-tb strain was isolated from the soil sample having tolerance level up to 400 mM of Cs^+. CsT-tb strain has ability to sorb Cs^+ from the solution which is relatively low in comparison to other bacteria. It confirmed the tolerance mechanism of high tolerance level bacteria toward Cs by maintaining intracellular Cs concentration. Silt and clay soil fraction treated by CsT-tb strain showed Cs desorption enhancement comparable with the acid treatment. The Cs sorption from solution and Cs desorption enhancement from soil by CsT-tb strain showed an interesting property for further bioremediation and understanding of Cs movement in the environment. From the phylogenetic tree of the 16S rDNA, the CsT-tb strain was closely related to *Bacillus* sp.

IV-5. References

1) International atomic energy agency (IAEA): Collection and preparation of bottom sediment samples for analysis of radionuclides and trace element. IAEA, Vienna (2003).
2) Laceby, J.P., et al., Journal of environmental radioactivity 183: 742-753 (2016).
3) Kurihara, M., et al., Journal of environmental radioactivity 187:81-89 (2018).
4) Bonnett, P. J. P., Journan of Environmental Radioactivity, 11:251–266 (1990).
5) Atarashi-Andoh, M., et al., Journal of environmental radioactivity 147: 1-7 (2015).
6) Hayashi, S., Global Environmental Research, 20:45–52 (2016).
7) Komissarov, M. A. and Ogura, S., Eurasian Soil Science, 50:861–871 (2017).
8) Basuki, T. et al., Journal Radioanalitycal Nuclear Chemistry, 316: 1039 (2018).
9) Wendling L. A. et al., Environmental Science and Technology., 39, 4505-4512 (2005)
10) Hinsinger P. et al., Journal of Soil Science, 44, 525-534 (1993)
11) Funari V. et al., Waste Management 60, 397–406 (2017)
12) Schauer, M., et al., Aquatic Microbiology and Ecololgy, Vol.31:163-174 (2003)
13) Dekker L. et al., FEMS Microbiol Letter, 359, 81–84 (2014)
14) Chino M., et al., Scientific Reports, 6:31376 (2016).
15) Korsakissok, I., et al., Atmospheric environment 70: 267-279 (2013).
16) Kitamura, A. et. al., Anthropocene 5:22–31 (2014).
17) Koarashi, J., et. al., The science of total environment 43:392-401 (2012).
18) Sato, K. et al., Journal of Physical Chemistry C 117:14075–14080 (2013).

19) Tsujimoto, M., et al. , Radiation Safety Management 15:1–4 (2016).

20) Avery S. V. et al., Journal of Industrial Microbiology, 14, 76-84 (1995)

21) Jung K. et al., Journal of Bacteriology,183:3800–3 (2001)

22) Kato S. et al., Scientific report, 6: 20041 (2016)

23) Heuck S. et al., Yeast. 27:817–35 (2010).

24) Diep P. et. al., Bioengineering and Biotechnology, 6:157 (2018)

25) Swer P. B. et al. AMB Express (2016) 6:69 (2016)

26) Qi et al., Journal of Experimental Botany, Volume 59, Issue 3 (2008)

27) Leyval C. and Berthelin J., Soil Science Society of America Journal, 55, 1009-1016 (1991)

28) Tomioka N., Uchiyama H., Yagi O, Applied and Environmental Microbiology, Vol 60 No 7: 2227-2231 (1994).

Chapter V

^{137}Cs soil to sediment ratio for investigation of ^{137}Cs migration from sloped forest catchment[1]

[1] Investigation of radiocesium migration from land to waterbody using radiocesium distribution and soil to sediment ratio: A case of the steep sloped catchment area of Ogi reservoir, Kawauchi Village, Fukushima

T. Basuki, W. C. Bekelesi, M. Tsujimoto, S. Nakashima, *Radiation Safety Management*, 19, (2020) 23-34. DOI 10.12950/rsm.190924

V-1. Introduction

The Fukushima Daiichi Nuclear Power Plant (FDNPP) accident that occurred on March 15, 2011 has caused radioactive materials released to the environment. The migration of FDNPP accident-derived radiocesium in terrestrial environment over years is key to the assessment of the long-term radiation hazard risk and its countermeasures.

The soil-water body migration from forest catchment is the important feature in Fukushima because the forest area covers more than 60% of the contaminated zone and has higher radiocesium inventory in comparison to the other land use. 2, 3) The forest area could be a long-term source of particulate radiocesium for the downstream area especially for the water body such as river, reservoir or lake and sea. 2,4)

The methods to estimate the migration of ^{137}Cs in catchment were difficult and time consuming such as by field experiment that utilized the leachate or seepage water samples and by measuring the ^{137}Cs in suspended solid of water sample. 3,5) Another method is by analyzing the vertical profile of the lake sediment. The idea is constructed by assuming that the catchment-derived ^{137}Cs has significant contribution to the total ^{137}Cs inventories in the lake sediment cores. 6) The relatively easier method of estimation was by using ^{137}Cs soil to lake sediment ratio to estimate the ^{137}Cs initial accumulation and flushing in the sediment of the lake just after the accident, however, it needs more investigation regarding its robustness. 7)

In this chapter, we examined the ^{137}Cs soil to lake sediment ratio for investigating the radiocesium migration from catchment to water body. We calculated the ratio using our data and previous research data and compared them.

V-2. Methodology

V-2.1. Soil and sediment sampling, sample preparation and measurement

The study area is in Ogi reservoir catchment area, Kawauchi village, Fukushima, that is located about 18 km southwest from FDNPP. Soil and sediment core sampling was conducted during March 15~16, 2018 in a steep sloped forest and transition zone of the catchment area and deeper part of the reservoir.

The soil and sediment core samples were cut each 2 cm and 1 cm increment, respectively. The samples were dried at room temperature and further dried by oven (105° C, 24 hours). The prior dry sieving (2 mm sieve) by electric horizontally rotating sieve (SKH-01, AS ONE) with mesh size 2 mm at about 280 rpm for 1 h was conducted to separate gravel and stone from the sample. The remaining samples were packed into so-called U8 vessel (100 ml, 5 cm height, 5 cm diameter) for radioactivity measurement.

The activities of ^{137}Cs were measured by gamma spectroscopy with HP Ge detector and multichannel analyzer (GEM 30-70, ORTEC), at energy peak of 662 keV.

V-2.1. ^{137}Cs soil to sediment ratio calculation.

The ^{137}Cs soil to sediment ratio was simply calculated by dividing the mean value of ^{137}Cs inventory of soil by that of sediment. The calculated ratio of the present study was compared with the ratio that is calculated based on the ^{137}Cs in soil and sediment data of previous studies in Fukushima area.[8, 9,10)] Location and time dependences of ^{137}Cs inventory in soil and sediment and its ratio were analyzed.

V-3. Results and Discussions

Table V-3.1. shows the data of ^{137}Cs inventory in soil and sediment and its ratio for some water bodies in Fukushima area. The previous and the present study are compared and further presented in Figure V-3.1. [7,8,10)]

Figure V-3.1.a. shows the comparison of ^{137}Cs inventory in soil and sediment of some water bodies along its distance from FDNPP. It shows the location dependence of ^{137}Cs inventory in soil and sediment for some water bodies. The higher ^{137}Cs inventory was found in the water body area closer to FDNPP. However, there was no location dependence in the case of ^{137}Cs inventory in soil to sediment ratio.

Figure V-3.1.b. shows the comparison of ^{137}Cs soil to sediment ratio for some water bodies along its sampling time. It shows that the ratio for the sample of longer sampling time from the accident is relatively smaller than that of the sampling time closer to the accident. The large variation among the data was most probably caused by the different characteristics of the catchment and water body, such as water ressident time and particle size of the sediment. [7)] The characteristics probably governed the migration and accumulation of ^{137}Cs. In the case of ^{137}Cs inventory in soil and sediment ($Bq\cdot cm^{-2}$), there was no time dependence.

Table V-3.1. Comparison of ^{137}Cs in soil, sediment and its ratio between the previous studies and the present study. The ^{137}Cs inventory value is decay corrected to each sampling date

Water body	Type	Location	Area (km^2)	^{137}Cs inventory in surrounding soil (Bq·cm^{-2})	^{137}Cs inventory in sediment (Bq·cm^{-2})	^{137}Cs soil to sediment ratio	Sampling date	References
Oyado	Irrigation pond	Nihonmatsu city, 40~50 km from FDNPP	0.001	36	8.2	4.4	July, 2011	Yoshimura et. al., 2014.
Takayashiki			0.001	32	42	0.75		
Neppami-Ike		Kawamata town, 40~50 km from FDNPP	0.002	35	6.6	5.3	August, 2011	
Matsuzawakami-ike			0.009	21	7.5	2.8		
Suzuuchi	Irrigation pond	Okuma town, ~10 km from FDNPP	0.004	640 ± 220	1300 ± 650	0.49 ± 0.30	July, 2016	Wakiyama et. al., 2017
Funasawa			0.011	290 ± 90	890 ± 630	0.33 ± 0.25		
Inkyozaka			0.007	210 ± 110	160 ± 67	1.3 ± 0.9		
Kashiramori			0.008	90 ± 40	110 ± 46	0.82 ± 0.34		
Hibara lake	Lake	Yama gun, ~100 km from FDNPP	10.8	0.30 ± 0.15	1.2 ± 0.5	0.25 ± 0.23	August, 2016	Basuki et. al., 2018.
Ogi	Reservoir	Kawauchi village, ~18 km from FDNPP	4.20	54 ± 10	100 ± 60	0.53 ± 0.31	March, 2018	Present study

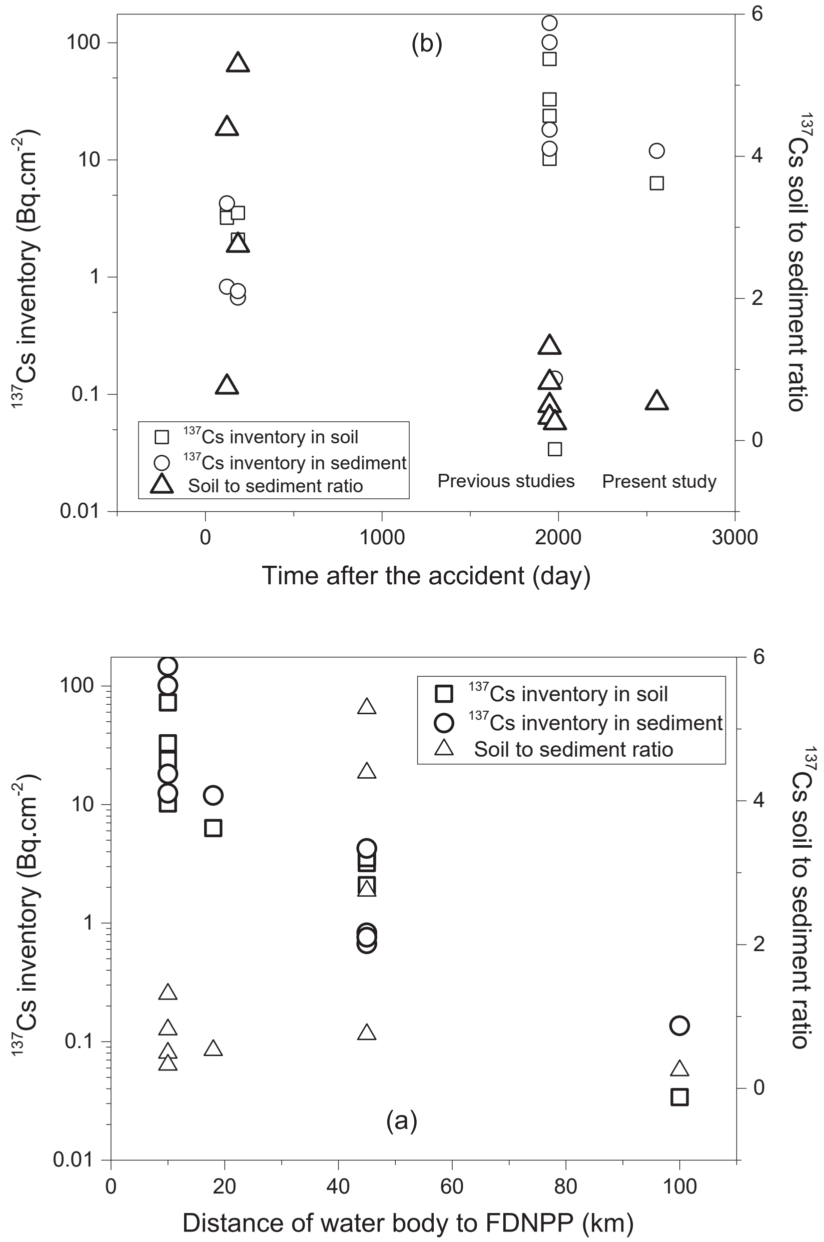

Figure V-3.1. Location dependency of ^{137}Cs inventory, the data are decay corrected to the released day (a), Time dependency of ^{137}Cs soil to sediment ratio, the data are decay corrected to the sampling day (b), of the present and the previous studies.

The radiocesium accumulation in sediment showed the low value of radiocesium soil to sediment ratio (0.53±0.31), see Table V-3.1., which means the higher radiocesium inventory in sediment than in soil catchment. Furthermore, the radiocesium soil to sediment ratio of the present study was lower than some previous studies, suggesting the time dependent accumulation.

The ^{137}Cs soil to sediment ratio of the present study was related to some previous studies, by neglecting the location and characteristics of the water body. The radiocesium soil to sediment ratio data of the present study and previous studies showed time dependency instead of location dependency, see Figure V-3.1. Although there are the large variation of the ratio among the data which was probably caused by the different characteristics of the catchment and water body, such as water resident time and particle size of the sediment. It has been explained before that longer resident time of water body and fine particle in the sediment will promote the radiocesium retention and accumulation in the sediment. The higher radiocesium retention and accumulation in the sediment will lower the radiocesium inventory of soil to sediment ratio. 7)

The radiocesium soil to sediment ratio was decreased sharply at time closer to the accident, however, the ratio was relatively stable or smaller decrease after long time from the accident, see Figure V-3.1.b. It could mean that there was a high rate of ^{137}Cs migration just after its deposition and the rate was decreasing with an increase of time. It was because the deposited Cs on the ground at the beginning was in the dissolved form, but later after the Cs interacted with the soil particles, the Cs was in the fixed form so that the Cs migration rate became slower. 11)

V-4. Conclusions

The low value of ^{137}Cs soil to sediment ratio provided the evidence of ^{137}Cs accumulation in the sediment from the soil catchment. The time dependency of ^{137}Cs soil to sediment ratio might show its potential to be used for investigating ^{137}Cs migration from catchment to waterbody.

V-5. References

1) International atomic energy agency (IAEA): Collection and preparation of bottom sediment samples for analysis of radionuclides and trace element. IAEA, Vienna (2003).

2) Laceby,J. P. et al., Journal of environmental radioactivity 183: 742-753 (2016).

3) Kurihara, M. et al., Journal of environmental radioactivity 187:81-89 (2018).

4) Koarashi, J. et al., Science total environment 43:392-401 (2012).

5) Nakanishi, T. et al., Journal of environmental radioactivity 128: 9-14 (2014).

6) He Q. et al., Chemical Geology, 129:115–131 (1996).

7) Yoshimura K. et al., Scientific reports, 4: 4514 (2014).

8) Basuki, T. et al., Journal of Radioanalitical and Nuclear Chemistry, 316: 1039 (2018).

9) Taira, Y. et al., PLoS ONE 7(9): e45816 (2012).

10) Wakiyama, Y. et al., Journal of Environmental Radioactivity 178-179 (2017).

11) Konoplev, A. V. et al., Analyst, June, Vol. 117 (1992).

Chapter VI

Air dose rate to ^{137}Cs ratio for predicting future air dose rate derived from ^{137}Cs inventory[1]

---

[1] Air dose rate to ^{137}Cs activity per unit area ratio for different land use 7 years after the nuclear accident -Case of the sloped catchment, Ogi reservoir, Fukushima-

T. Basuki, W. C. Bekelesi, M. Tsujimoto, S. Nakashima, *Radiation Measurements* (2020). https://doi.org/10.1016/j.radmeas.2020.106424

VI-1. Introduction

A significant amount of radioactive materials was released into the environment during the Fukushima Daiichi Nuclear Power Plant (FDNPP) accident that occurred on March 2011. Ground contamination in the Fukushima area is one of the main concerns, in addition to marine ecosystem contamination. Ground contamination in this area initially comprised of relatively large amounts of some highly volatile radionuclides such as ^{131}I, ^{134}Cs, ^{137}Cs and ^{132}Te , and relatively small amounts of mildly volatile elements such as ^{89}Sr and ^{90}Sr, with trace amounts of low volatile radionuclides such as ^{238}Pu, ^{239}Pu and ^{240}Pu. These radionuclides have widely varying half-lives.1) and some of them are gamma emitters that contribute to the ambient equivalent dose rate in air (air dose rate). However, considering the physical half-life of the radionuclides, ^{137}Cs with a 30.2-year physical half-life is the key contributor to air dose in the long-term.2,3)

The contribution of ^{137}Cs to the air dose rate has been analyzed in the cases of nuclear weapon tests and the Chernobyl accident.2,3,4) The understanding on the relationship between the air dose rate and the ^{137}Cs activity per unit area in the soil is highly important to examine ^{137}Cs migration to predict future dose rates, and to evaluate the remediation strategies.5) It has been shown that the ratio of the air dose rate to the ^{137}Cs activity per unit area decreased with time after the deposition up to 3 years3) and up to 10 years 2) and less changeable after that period.

^{137}Cs migration has been investigated as one of the factors that might affect the contribution of ^{137}Cs to the total air dose rate. Very complex factors were found to influence the migration behavior of radionuclides. Previous studies have considered the type of land use as one of the key factors affecting the relationship between the air dose rate and ^{137}Cs activity per unit area for both undisturbed area (forest area, grass land etc.) and disturbed area (farmland, housing area etc.). In the case of forest area, there is a time-dependent radionuclide flux from forest canopies to grounds in forest areas. 6,7) The vertical migration of radiocesium into deeper regions of soil also depends on the land use type. For example, radiocesium was penetrated deeply in soil of forest area than that of more open area, due to the role of litter layer and organic matter rich soil of forest area, even though the litter layer was also capable to retain the radiocesium. 8) The migration behaviors combined with the physical half-life of ^{137}Cs influence the ratio of the air dose rate to the ^{137}Cs activity per unit area.

However, there is a lack of understanding regarding this relationship considering the land use type factors. Furthermore, an extremely limited number of analysis has been performed on the influence of ^{137}Cs vertical migration to the relationship in the Fukushima area after the accident.

In this chapter, we analyzed the ratio of the air dose rate to the ^{137}Cs activity per unit area in the case of different land uses in the Fukushima area after the FDNPP accident, and compared the obtained data with those from previous studies. The ratio data are expected to play a key role in estimating the future air dose rate of specific locations and will also contribute to the evaluation of decontamination activities after nuclear accidents.

VI-2. Methodology

VI-2.1. Air dose rate measurement, sampling and sample measurement.

The air dose rate measurement and soil sampling campaign were conducted on 15~16 March 2018 in sloped catchment of Ogi reservoir, Kawauchi village, Fukushima. The air dose measurement was conducted by survey meter with NaI detector (ALOKA MYRATE PDR-111) 1 m above the ground. The survey meter has been periodically calibrated using standard source and standard survey meter.

The triplicate of soil sample was collected by hand core sampler (25 cm long tube, 19.6 cm^2 area) inside the grid, following the previous work. 3) The measurement and sampling grid were selected purposively within study area, that consisted of forest area, transition zone (no vegetation) and farmland.

^{134}Cs, ^{137}Cs and terrestrial naturadionuclides (TNRs) were measured by gamma spectrometer with HP Ge detector. The air dose rate contributed from TNRs was calculated by using methodology that has been explained in Chapter 2.

VI-2.1. Air dose rate to ^{137}Cs inventory ratio calculation.

Air dose rate to ^{137}Cs inventory ratio was simply calculated by dividing the mean value of measured air dose rate by ^{137}Cs inventory from the same location. The error value was obtained from the standard deviation. The ratio that is calculated from some previous research data was compared with the present study data.2-4, 9,10)

VI-3. Results and Discussions

VI-3.1. Radiocesium inventory and air dose rate for different land use.

Table VI-3.1. summarizes the measured air dose rate, ^{134}Cs and ^{137}Cs activity per unit area, air dose rate to ^{137}Cs activity per unit area ratio, and air dose rate from TNRs for different land use types.

The relationship between the air dose rate and the ^{137}Cs activity per unit area is illustrated in Figure VI-3.1. The air dose rate increases with the increase of ^{137}Cs activity per unit area. This indicates that ^{137}Cs contributes to the air dose rate, in addition to background radiation and ^{134}Cs.

Large variations in the air dose rate and radiocesium activity per unit area were observed among the different land use types, with a higher air dose rates and radiocesium activity per unit area in the forest areas. Higher radiocesium retention was also observed in the forest areas, compared to the open areas with no vegetation areas (transition zones) and farmlands. These results are in agreement with those of previous studies. 11,12)

Furthermore, the radiocesium activity per unit area exhibited large variations among the samples collected from very narrow sampling grids. In other words, the radiocesium might be redistributed in small areas after deposition.[13] This reveals that the sampling should be performed in a way that representative samples even for very narrow sampling grids are collected. Conversely, the air dose rate 1 m above the ground exhibited a low variation in the small-scale sampling grids, where the measured photons contributions from sum of complex radiation point sources in the environment.

The ^{134}Cs activity per unit area was roughly 10 times smaller than the ^{137}Cs activity per unit area for all land use types, as observed in Table VI-3.1., owing to its short physical half-life. Considering this fact, the contribution of ^{134}Cs to the air dose rate will be negligible in the long term, even though ^{134}Cs has a dose conversion ratio roughly 2.7 times higher than that of ^{137}Cs.[9)]

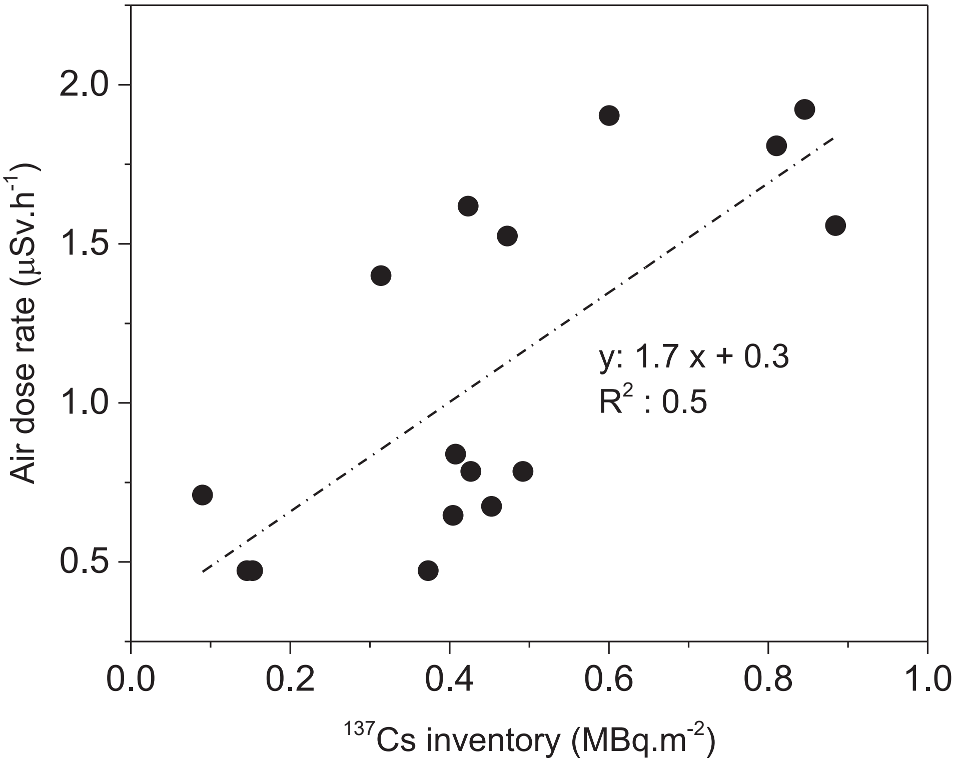

Figure VI-3.1. Correlation between ^{137}Cs activity per unit area and air dose rate for different land use.

Table VI-3.1. Air dose rate, ^{137}Cs, ^{134}Cs inventory, air dose rate to inventory ratio, and air dose rate from TNRs for different land use. ^{137}Cs and ^{134}Cs were decay corrected to sampling day on March 16, 2018

Area	*n*	Air dose rate (μSv/h)		^{134}Cs inventory (MBq/m^2)		^{137}Cs inventory (MBq/m^2)		Air dose to ^{137}Cs inventory ratio ([μSv/h]/[MBq/m^2])		TNRs contributed Air dose rate (μSv/h)	
		Mean	Err (±)[a]	Mean	Err (±)[a]	Mean	Err (±)[a]	Mean	Err (±)[a]	Mean	Err (±)[a]
Area 1, forest	3	1.71	0.19	0.06	0.02	0.66	0.42	2.6	0.9	0.06	0.03
Area 2, forest	4	1.65	0.10	0.05	0.01	0.60	0.39	2.8	0.6	0.04	0.02
Area 3, no vegetation	3	0.68	0.02	0.03	0.01	0.32	0.51	2.1	1	0.06	0.04
Area 4, Farmland	3	0.47	0.06	0.02	0.01	0.22	0.52	2.1	0.9	0.09	0.05

[a] Standard deviation

Table VI-3.2. Air dose to ^{137}Cs ratio collected from previous researches data

References	Source of fall out	Site	Measurement time from the deposition (year)	Land use type	Air dose rate to ^{137}Cs inventory ratio ([μSv.h^{-1}]/[MBq.m^{-2}])
K.M., Miller at al., 1990.	Mainly from nuclear weapon test	Northeastern US	25	Forest	1.3[a]
				Un-disturb non forest	0.73[a]
V., Ramzaev et al., 2005	Mainly from Chernobyl nuclear accident	Bryansk region, Russia	17	Forest	1.4[a]
				Un-disturb grassland	1.3[a]
D.N., Timms et al., 2004	Mainly from Chernobyl nuclear accident	Svyatoye lake-Catchment, Belarus	14	n.a.	1.2[a]
MEXT, 2012	Fukushima accident	Fukushima area	1	n.a.	3.6
S., Mikami et al., 2019	Fukushima accident	Fukushima area	1~5	n.a.	2.6

n.a. : not available

[a] The data was converted from absorbed dose rate (nGy/h) to ambient dose equivalent rate (nSv/h) by factor 1.2.

VI-3.2. ^{137}Cs vertical profile in soil for different land use.

Figure VI-3.2.a. shows the vertical profile of ^{137}Cs relative activity per unit area (%) and Figure VI.3.2.b. shows the vertical profile of ^{137}Cs activity concentration (kBq·kg^{-1}) in the soil for the different land use types. It can be observed from the Figure VI-3.2.a. that ^{137}Cs in the forest soil penetrated relatively deeply in comparison to the soil with no vegetation (transition zone). The relatively deeper penetration of ^{137}Cs in forest soil is consistent with the findings of previous studies. 7,8) Deeper penetration depth of ^{137}Cs in forest soil occurred in the litter layers and organic matter rich soil layers of the forest floor, however, a significant portion of ^{137}Cs was still retained in the litter layer of forest. 8) Furthermore, ^{137}Cs from litter layer and organic matter rich layer of forest soil was relatively immobilized when it reaches the mineral layers of the forest soil. 7)

Furthermore, Figure VI-3.2.a. shows that more than 75% of ^{137}Cs is still located in shallow soil (< 20 kg·m^{-2} or < 4 cm physical depth) for both the forest area and transition zone. The results are not consistent with the previous investigation that shows more ^{137}Cs in surface soil of forest area than more open area. 2) The reason of the difference may reflect the difference of the sampling time from the deposition time, i.e., the study by Miller et al. (1990) was conducted about 25 years after the deposition and the present study was conducted 7 years after the deposition. Another reason of the difference was the difference in the soil component, but this is still under study. For the farmland, the vertical profile of ^{137}Cs in soil showed a relatively homogenous vertical distribution, owing to ploughing and vertical migration. Figure VI-3.2.a. also shows that more ^{137}Cs migrated to deeper soil region of deciduous forest than coniferous forest. This implies that the deeper penetration of radiocesium in forest soil may not be a universal observation that depends on forest tree species that may be influenced the organic matter content in the forest soil. Different ^{137}Cs vertical profile among different forest type is previously shown. 8)

Figure VI-3.2.b. shows the vertical profile of ^{137}Cs activity concentration in the soil. Very low activity concentration of ^{137}Cs was found on the surface soil of the transition area, which may be related to soil erosion. The lowest ^{137}Cs concentration was found in the farmland, owing to decontamination activities.

VI-3.3. The air dose rate and radiocesium inventory: forest canopy, soil shielding and elapsed time effect.

The ratio of the air dose rate to radiocesium activity per unit area for different land use types is presented in Table VI-3.1. The ratio tends to be higher in forest areas than in open areas and farmlands, and this finding is consistent with some previous reports that are shown in Table VI-3.2.

This tendency of the higher ratio of the forest area than open area and farmland can be attributed to various factors. The continuous influx of radiocesium from the forest canopy to the forest floor might have contributed to the higher ratio, although it was found that the amount of radiocesium attached to the canopy of the Fukushima forest has decreased after 2013.6) This could imply that ^{137}Cs source was mostly in the forest soil. On the other hand, a coniferous forest near Iwaki, Fukushima showed 10-40% of the radiocesium activity in 2013 remained in the forest canopy, although it contributed only <5% to the total air dose rate owing to its distance from the detector.16)

Another plausible factor of higher ratio of forest area than more open areas was the location of ^{137}Cs in soil profile as a result of vertical migration. The shallower ^{137}Cs in soil will keep the distance of the radiation source closer to the detector and reduce the soil shielding effect. However, the effect of vertical migration to the ratio is not clearly shown in this study, maybe because that the soil shielding effect is negligible by considering more than 75% of ^{137}Cs is still in the soil surface of coniferous forest, deciduous forest and transition zone. The attenuation of air dose rate by shielding of soil will be less significant if the radiation source is located close to the soil surface.2) It is also reported that the count rate and total kerma from the same activity and depth in forests compared to grasslands were decreased by 19% 14) and by 20% 16), owing to the biomass above the soil in the forests. A continuous investigation with a longtime scale is needed to strongly conclude the effect of vertical migration to the ratio.

Table VI-3.2. presents the ratio data reported by previous studies. It shows the time dependency of the ratio, in which the measurement right after the deposition time had higher values than that in delayed measurements. The decrease in the ratio was due to the physical half-lives of the gamma emitter radionuclides and radionuclide vertical migration in the soil. By comparing the ratio data in Table VI-3.1. with that in Table VI-3.2., it is predicted that the ratio in the present data would be a relatively lesser decrease in the future as negligible influx of ^{137}Cs from forest canopy in longer time after the deposition and relative ^{137}Cs immobilization in the soil layer, especially in soil mineral layer. It is known that the radiocesium penetrates deeply in litter layers and organic matter rich soil of forest floor and is relatively immobilized once it reaches the mineral soil layers.7) Long-term studies on the derived ^{137}Cs and its ratio with the air dose rates have revealed that the ratio was less changeable after 10 years from the deposition2) and 3 years from the deposition.3)

VI-3.4. Contribution of terrestrial natural radionuclides (TNRs) to the air dose rate.

The activity of TNRs, which are important contributors to the natural background radiation, was measured, and their contribution to the air dose rate was evaluated. The contribution of TNRs to the air dose rate is presented in Table VI-3.1. The contribution of TNRs in coniferous forest areas, deciduous forest areas, transition zones (no vegetation), and farmlands to the air dose rate are 0.06±0.03 μSv/h, 0.04±0.02 μSv/h, 0.06±0.04 μSv/h, and 0.09±0.05 μSv/h, respectively. The results are in agreement with the previous research value about 0.05 μSv/h. [9] The contribution of natural radiation to the air dose rate in agricultural lands is relatively higher than in the other land uses. This is due to contribution by ^{40}K from anthropogenic sources such as fertilizers. These values, therefore, show a low contribution of TNRs to the air dose rate.

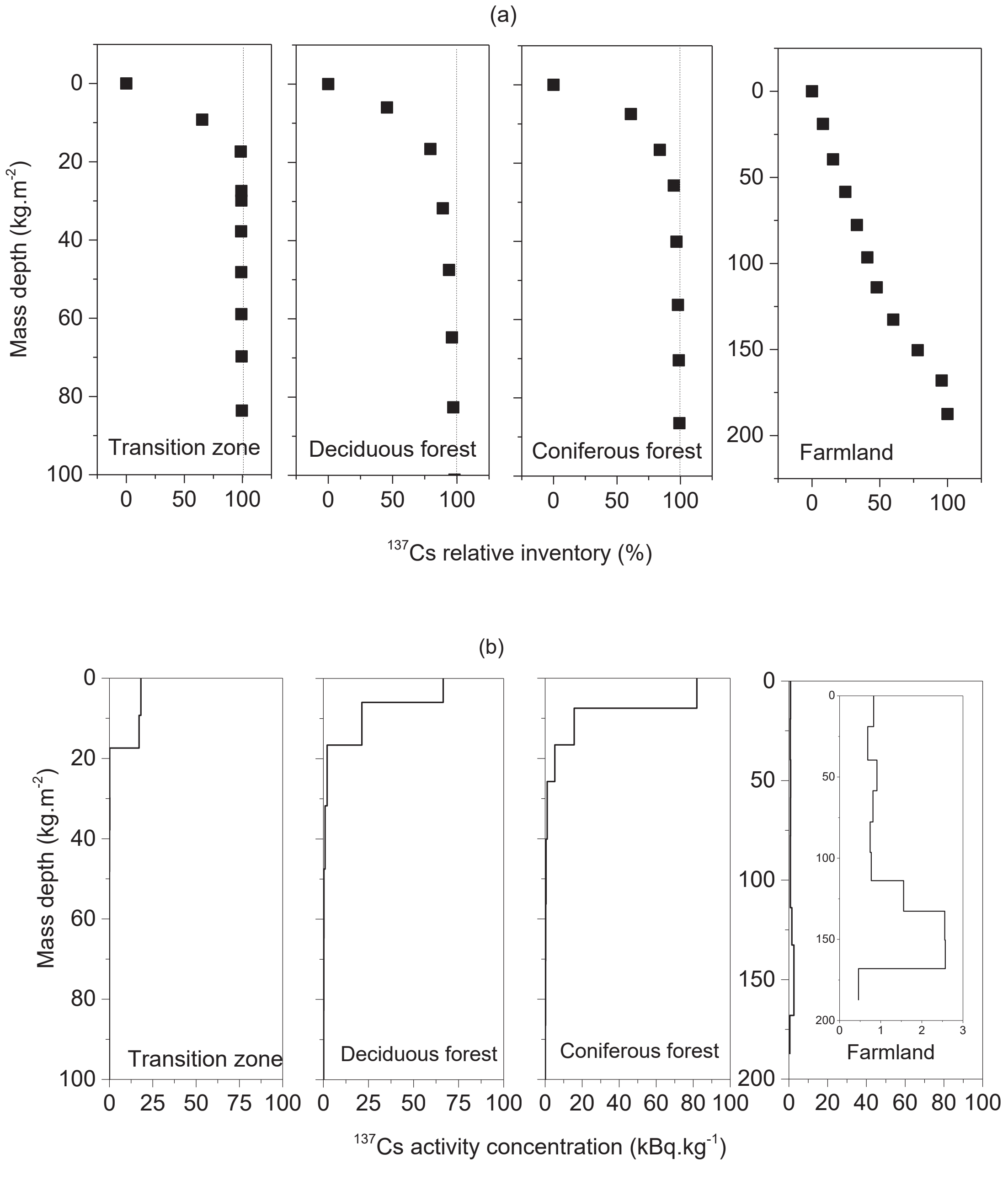

Figure VI-3.2. Relative ^{137}Cs inventory (%) (a) and activity concentration (b) against mass depth of the soil.

VI-4. Conclusions

We evaluated the ratio of the air dose rate to the ^{137}Cs activity per unit area in soil, seven years after the nuclear accident in Fukushima. The ratio was relatively higher in the forest area, compared to open areas. This was probably due to the continuous ^{137}Cs influx from the forest canopy for a while after the accident. The less influence of ^{137}Cs vertical migration in the forest soil profile to the ratio was shown, that might be a result of ^{137}Cs accumulation in the soil surface of undisturbed area. It was estimated that the ratio would decrease less in the future, owing to the decay out of shorter half-life nuclides and relative immobilization of ^{137}Cs in the ground.

VI-5. References

1) International Atomic Energy Agency (IAEA), 2015, The Fukushima Daiichi Accident: Technical Volume 1, Description and Context of the Accident. Vienna, Austria.

2) Miller, K. M., Kuiper, J.L., Heifer, I. K., Journal of Environmental Radioactivity, 1990, 12, 23-47.

3) Ramzaev, V., Yonehara, H., Hille, R., Barkovsky, A., Mishine, A., Sahoo, S. K., Kurotaki, K., Uchiyama, M., Journal of Environmental Radioactivity, 2005, 85, 205e227. doi:10.1016/j.jenvrad.2004.04.014.

4) Timms, D.N. Smith, J.T. Cross, M.A. Kudelsky, A.V. Horton, G. Mortlock, R. Journal of Environmental Radioactivity, 2004, 72, 323–334. doi:10.1016/S0265-931X(03)00219-4.

5) Malins, A., Kurikami, H., Kitamura, A., Machida, M., Health Physics., 2006, 111(4):357–366.

6) Imamura, N., Akama, A., Ohtani, Y., Kobayashi, M., Tsuboyama, Y., Takahashi, M., Journal of Japan Forest Society, 2017, 99: 1—9 (*in Japanese*).

7) Kurihara, M., Onda, Y., Kato, H., Loffredo, N., Yasutaka, T., Coppin, F., Journal of Environmenal Radioactivity, 2018, 187, 81-89. https://doi.org/10.1016/j.jenvrad.2018.01.027.

8) Koarashi, J., Andoh, M. A., Matsunaga, T., Sato, T., Nagao, S., Nagai, H., Science of the Total Environment, 2012, 431, 392–401. https://doi:10.1016/j.scitotenv.2012.05.041.

9) Mikami, S., Tanaka, H., Matsuda, H., Sato, S., Hoshide, Y., Okuda, N., Suzuki, T., Sakamoto, R., Andoh, M., Saito, K., Journal of Environmental Radioactivity, 2019, 210, 105941. https://doi.org/10.1016/j.jenvrad.2019.03.017.

10) Emergency Operation Center, Ministry of Education, Culture, Sports, Science and Technology (MEXT), 2012, Summarized Version of the “Results of the Research on Distribution of Radioactive Substances Discharged by the Accident at TEPCO’s Fukushima Dai-ichi NPP”. Japan.

11) Kitamura, A., Yamaguchi, M., Kurikami, H., Yui, M., Onishi, Y., Anthropocene, 2014, 5:22–31. https://doi.org/10.1016/j.ancene.2014.07.001.

12) Laceby, J. P., Huon, S., Onda, Y., Vaury, V., Evrard, O., Journal of Environmental Management, 2016, 183, Part 3, P 742-753. https://doi.org/10.1016/j.jenvman.2016.09.020.

13) Bonnett, P. J. P., Journal of Environmental Radioactivity, 1990, 11:251–266. https://doi.org/10.1016/0265-931X(90)90018-Q.

14) Gering, F., Kiefer, P., Fesenko, S., Voigt, G., Journal of Environmental Radioactivity, 2002, 61, 75–89.

15) Sanderson , D. C. W., Cresswell , A. J., Tamura , K, Iwasaka , T, Matsuzaki, K, Journal of Environmental Radioactivity, 2016, 162-163:118-128, doi: 10.1016/j.jenvrad.2016.05.019.

16) Cresswell, A., Kato, H., Onda, Y., and Nanba, K., Journal of Environmental Radioactivity, 2016, 164, pp. 133-144. https://doi.org/10.1016/j.jenvrad.2016.07.024.

Chapter VII

General Conclusions

We showed that the silt and clay fraction (size <75 μm) hold dominantly the radiocesium than other fractions. The highest activity concentration on silt and clay fraction was always found at the peak layer. It probably shows that the silt and clay fraction was a medium of radiocesium migration from catchment to water body.

We showed high retention of ^{137}Cs in the steep sloped forest area after 7 years from the accident. The migration of ^{137}Cs from catchment to reservoir was probably contributed more from the no vegetation area. The sediment vertical profile showed the accumulation of ^{137}Cs in the deeper layer of sediment. The physicochemical property of the forest surface soil could be a possible factor of high retention of radioactive contaminant in the steep sloped forest zone.

We showed that Cs was toxic for soil bacteria in general. Isolated Cs tolerant bacteria from soil showed to have Cs sorption capacity from solution and enhance Cs desorption from soil matric. It shows that soil bacteria may have a role in ^{137}Cs migration in the soil.

Time dependency of ^{137}Cs soil to sediment ratio was shown and it might be used for investigation of ^{137}Cs migration from forest catchment to water body.

We predicted that air dose rate to ^{137}Cs inventory ratio will be less changeable in the future, so that, it can be used for long-term dose assessment derived from ^{137}Cs inventory.

Acknowledgement

It is the time for me to look back to a wonderful 5 years journey of study in Hiroshima University. A best time in my life, that finally brought me to know more about our wonderful world, science, research and academic life, to realize how important my family is, how great, wise and kind my Professor in teaching me, and the most important thing is I know more about myself and my Creator, God almighty, Allah swt.

I would like to express my very deep gratitude to my supervisor, Professor Satoru NAKASHIMA. I do not know how to thank to you for everything you have given to me and my family. I always said to my children when we had a talk, you are a man with a golden heart.

I would like to thank to Phoenix leader education program Hiroshima University, Graduate School of Science Hiroshima University and Oshimo Foundation for giving financial support during the study.

I would like to thank to all member of radioisotope center, Hiroshima University, especially Dr Sunao Miyashita and Dr Kuninobu Inada, who always help me to solve the technical problem during my experiment.

I would like to thank to my all Japanese friends, especially my all laboratory mate (Masaya Tsujimoto san, Naguwa san and others) and my friends from Phoenix leader education program (Mari Ishimori san, Hai san, Wiseman, Satrio, Herry, Habib and others) that made my study life become easier.

I would like to thank to my mentor Dr Tuswadi that has introduced me to the Phoenix leader education program, Hiroshima University and always given valuable advice for me.

Finally, I would like to thank to my family, my beloved wife Catur Widiasari, my children (Zaidan, Althaf, Mafaza), my parent (Agus Salim and Sulijah), my brother (Purbo Santoso) and my sister (Dwi Astuti). All of you are the reason why I never gave up and always fight to the end.